SYNTHESIS AND CHARACTERIZATION OF ZINC OXIDE NANOPARTICLES BY CHEMICAL METHOD

Submitted by

Rakesh Saroha

ROLL NO-11/NST/2K10

In partial fulfilment for the award of the Degree of

Master of Technology

IN

NANOSCIENCE & TECHNOLOGY

UNDER THE ESTEEMED GUIDANCE OF

Dr. Amrish K. Panwar

(Assistant Professor)

DEPARTMENT OF APPLIED PHYSICS

DELHI TECHNOLOGICAL UNIVERSITY (formerly DCE)

SHAHBAD DAULATPUR, BAWANA ROAD, DELHI-110042

DEPARTMENT OF APPLIED PHYSICS

DELHI TECHNOLOGICAL UNIVERSITY (formerly DCE)

SHAHBAD DAULATPUR, BAWANA ROAD, DELHI-110062

CERTIFICATE

This is to be certify that the thesis entitled, "*Synthesis and characterization of ZnO nanoparticles from chemical method*" submitted by Mr. Rakesh Saroha (2k10/11/NST) in fulfilment for the requirements for the award of Master of Technology degree in Nano Science & Technology, Delhi Technological University is an authentic work carried out by him under my supervision and guidance. To the best of my knowledge, the matter embodied in the thesis has not been submitted to any other University / Institute for the award of any Degree or Diploma.

Date………

Dr. Amrish K. Panwar   **Prof. S. C. Sharma**

Department of Applied Physics   Head of the Department

Delhi Technological University (formerly DCE)

DECLARATION

I hereby declare that the work which is being presented in this dissertation entitled *" Synthesis & Characterization of ZnO nanoparticles "* submitted to the Department of Applied physics, Delhi Technological University in fulfillment of the requirement of the degree of **Master of Technology (Nanoscience & Technology)** is an authentic record of my own work done under the guidance of **Dr. Amrish K. Panwar**, Assistant Professor, Delhi Technological University, New Delhi-110042.It is an original work and matter embodied in this dissertation has not been previously submitted for the award of any degree elsewhere.

Date……………….

Rakesh Saroha

Roll No- 11/NST/2K10

M.Tech Nanoscience and Technology

Delhi Technological University

New Delhi

<u>ACKNOWLEDGEMENT</u>

I have taken efforts in this project. However, it would not have been possible without the kind support and help of many individuals and organizations. No amount of words can adequately express the debt I owe to my Guide, **Dr.Amrish K. Panwar**, Assistant Professor, Department of Applied Physics, D.T.U for his continuous encouragement and thoughtful discussion during the course of present work. I am very grateful to him for giving me the opportunity to work on metal oxide, appreciating my ideas and allowing me the freedom to take on the tasks independently, helping me to explore the things by myself and enriching me with the knowledge amassed.

I am highly indebted **to Dr. Pawan K. Tyagi**, for providing me necessary equipments regarding the project work & also for their support in completing the project.

I would like to express my special gratitude and thanks to our research scholars **Mr. Vinay**, **Miss Lucky**, **Mrs. Ritu**, for giving me such attention and time.

I take this opportunity to express my deep sense of gratitude towards **Mr. Aman**, **Mr**. **Sandeep** for helping me a lot in my characterization work.

Finally, yet importantly, I would like to express my heartfelt thanks to my beloved parents for their blessings, all my friends / classmates for their help and wishes for the successful completion of this project.

Date…………..

<div align="right">

Rakesh Saroha
Roll No- 11/NST/2K10

M.Tech Nanoscience and Technology

Delhi Technological University

New Delhi

</div>

ABBREVATIONS

1. Nanometer-- nm

2. X-ray Diffraction--XRD

3. Scanning Electron Microscope--------------------------------------SEM

4. Tunneling Electron Microscope--------------------------------------TEM

5. Scanning Tunneling Microscope------------------------------------STM

6. Differential Scanning Calorimetry----------------------------------DSC

7. Thermal Gravitometry--TGA

8. Fourier Transform Infrared Spectrosopy----------------------------FTIR

9. Ultraviolet-visible Spectroscopy------------------------------------UV- vis

10. Physical Vapour Deposition---PVD

11. Chemical Vapour Depositon--CVD

UNITS

1.   Nanometer---10^{-9} meter

2.   Electron volt---1.6×10^{-19} Joule

3.   Angstrom--10^{-10} meter

List of Figures   Page No.

Contents   Page No

Chapter 4

4. CHARACTERISATION TECHNIQUES

Chapter 5

5. RESULT AND DISCUSSION

Chapter 6

Chapter 6

Abstract

The ZnO nanoparticles were successfully synthesized by chemical method were found to be (20-70) nm in size as revealed by XRD Scherer's formula. The particle size measurement was done by SEM, TEM. In the present research work ZnO nanoparticles were synthesized using Zinc Acetate in ethanol with further addition of ethyl acetate. The white synthesized ZnO powder was then heated at 450℃, 750℃ and 900℃ temperatures. The ZnO samples were then characterized by XRD, SEM and TEM. Further characterization was done using FTIR, UV- visible spectroscopy and DSC-TGA. The hexagonal wurtzite structure of ZnO was confirmed by XRD spectra. FCC structure was also predicted by the XRD peaks. The optical properties of the ZnO samples were studied by UV-visible spectroscopy. The temperature variation of samples indicates that the size increases with increase in temperature while the XRD peaks gets sharper and sharper. The thermal properties were investigated by TGA.

Chapter 1

INTRODUCTION

1.1   Motivation and Background For The Project

Today, in the age of science technology and innovation when world is surmounting on the roof of technology & electronics mostly dominated by miniaturize devices and electronic equipments and thereby creating the need of new materials and technologies into all aspects of daily life. Since the early -1960s the potential of integrated circuits that are used in the computer industry has grown exponentially fulfilling a prediction by Gordon E. Moore, called 'Moore's law'. In order to fulfil this prediction very common type of material comes out that is "semiconductor". These semiconductors mainly dominated by known elements Gallium (Ga), Indium (In), Silicon (Si) and Germanium (Ge) which makes their way in the periodic table as p-block elements. The starting point of the semiconductor industry was the invention of the first semiconductor transistor at Bell Lab in 1947. Germanium which possesses properties like low melting point and silicon dominates the commercial market for its better fabrication technology and application to integrated circuits. As time passes on the rapid growing world demands speed with technology which was fulfilled by a compound semiconductor Gallium Arsenide (GaAs) which makes it easy for high speed optoelectronic devices. As compare to silicon Gallium Arsenide which does a direct band gap semiconductor possess higher carrier mobility along with higher effective carrier velocity which makes it better suited for optoelectronics devices. But for high temperature electronic devices something more was required. Due to this world now demand a material with properties like high bad gap, higher electron mobility as well as higher breakdown field strength. So on making investigation the name of compound comes out is "Zinc Oxide" which is a wide band gap semiconducting material having high electron mobility, high thermal conductivity, wide and direct band gap, and large exciton binding energy [1, 3, 12, 58] which makes it suitable for wide range of devices, including transparent thin-film transistors, photo detectors,   light emitting diodes and laser diodes that operates in the blue and ultraviolet region of the spectrum. Also zinc oxide has been commonly used in its polycrystalline form over hundred years in a wide range of applications. It creates enthusiasm to develop proper growth and process technique for synthesis of zinc oxide. Zinc Oxide is also known as "Lu-Gan-Stone " in china, Zinc oxide has been In used in medical treatment for quite number of years in china.

In the last decade world witnessed a rapid action in the research related to zinc oxide as a semiconductor. From the 1960s, synthesis of ZnO thin films has been an active field because of their applications as sensors, transducers and catalyst .The decade of 1970 for ZnO away in manufacturing of simpler ZnO devices like ceramic varistors, piezoelectric transducers [2] etc. A lot of work on metallo-organic chemical vapour deposition has been done extensively in latter decade. Newer methods were used including pulsed laser deposition and moleculer beam epitaxy [3] in the 1990s which leads to commercial availability of ZnO. In the last decade a lot of research has been done to study the surface modification and photocatalytic property of ZnO [4, 50] and applications in low-voltage and short-wavelength electro-optical

devices, transparent ultraviolet protection Films, and spintronic devices [49]**.** Now researchers are investigating optical properties of ZnO capped with polymers [5] along with its piezoelectric properties [6]**.** ZnO has now become one of most studied material as it presents very interesting properties for optoelectronics and sensing applications, in nano range synthesis.

1.2   What Is NanoTechnology

According to a general accepted definition 'nanotechnology' is a technology concerned with objects that have at least in one dimension a size of less than 100 nm. This means that underlying 'nanophysics' can be placed between mesoscopic physics (the physics of objects between a few microns and one   hundred nanometer) and microscopic physics (the physics of interactions between individual atoms and molecules) [7].

The European Union as well as the large American and Japanese (and to a certain degree also Chinese, Brazilian, Indian etc.) research societies currently invest substantial resources in research geared towards applied nanotechnologies. One of the big expectations is that nanotechnology will eventually fulfil the dreams of scientists from all disciplines; from physicist waiting to see quantum mechanical concepts come to life; via chemist, longing to fabricate large molecules atom for atom; to biologists, seeking to control atom transport into and out of membranes and understand which functions the macromolecules composing the genome perform. "There's *plenty of room at the bottom",* as Richard Feynman stated as early as 1959.

Eric Drexler in the early 1980's coined the word "NanoTechnology"

1.3   History Of Zinc Oxide

It is hardly possible to trace the first usage of zinc oxide-zinc compounds were used by early humans, in processed and unprocessed forms, as a paint or medical ointment, but their composition was uncertain.

"*Pushpanjan*" probably zinc oxide was used for eyes and open wounds, is mentioned in the Indian medical text the "Charaka Samhita", thought to date from 500 BC or before [8]. Around 1st century AD it was used as a preferred treatment for a variety of skin conditions including skin cancer. It is still widely used in a variety of products such as baby powder, antiseptic ointment, anti-dandruff shampoos and creams against diaper rashes.

Around 200 BC Romans produced brass, an alloy of zinc and cooper by a cementation process where copper was reacted with zinc oxide, which is thought to have been produced by heating zinc ore in a furnace [8]. In India it has also been recovered from zinc mines at Zawar around 1st BC. From 12th to the 16th century zinc and zinc oxide were recognized and produced in India using a primitive form of the direct synthesis form.

In 17th century zinc manufacture moved to China from India. Zinc oxide was mainly used in paints and ointments [8]. This white powder was widely accepted as water cooler by 1830s but it did not mix well with oil. It was used by some artists as a base for their oil paintings in 1890s and 1900s, due to the fact that it makes a rather brittle dry film when unmixed with other colors. It was mostly used in rubber industry in the vulcanization of rubber. In recent times it was used in photocopying as it was added into the photocopying paper as a filter.

1.4   Processing methods of Nanomaterials

There are a large number of techniques available to synthesize different types of nanomaterials in the form of colloids, clusters, powders, tubes, rods, wires, thin films etc.There are therefore various physical, chemical, biological and hybrid techniques available to synthesize nanomaterials.

The technique to be used depends upon the material of interest, type of nanostructure viz. zero dimensional (0-D), one dimensional (1-D) or two dimensional (2-D) material, size, quantity [9] etc.
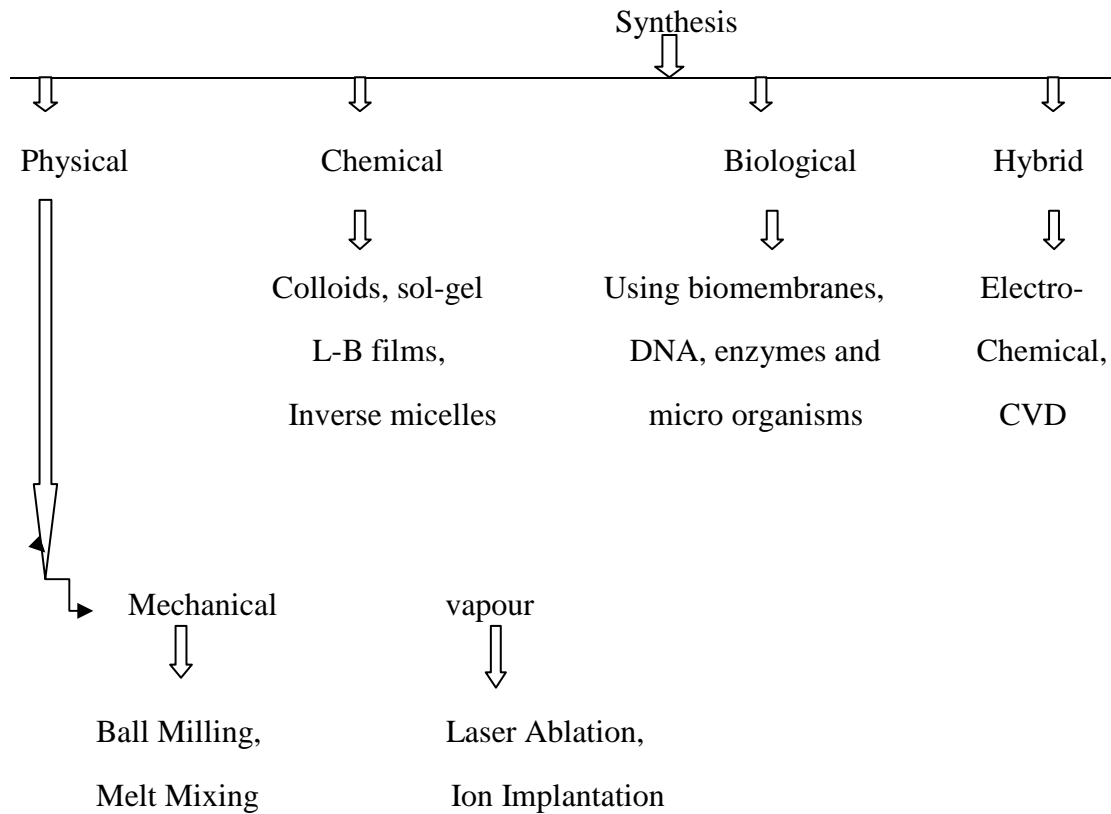
Synthesis

| Physical | Chemical | Biological | Hybrid |

Colloids, sol-gel

L-B films,

Inverse micelles

Using biomembranes,

DNA, enzymes and

micro organisms

Electro-

Chemical,

CVD

Mechanical   vapour

Ball Milling,   Laser Ablation,

Melt Mixing   Ion Implantation

Fig. 1.4.1: A Schematic Diagram of types of Synthesis of Nanomaterials

There are two different approaches of material fabrication. One is the "Top-Down" approach and the other is "Bottom-Up" approach. In the first one, generally a bulk material is taken and machined it to modify into the desired shape and product. Examples of this type of technique are the manufacturing of the integrated circuits using a sequence of steps such as crystal growth, lithography, Etching, ion implantation etc. For nanomaterial synthesis, ball-milling is an important top-down approach, where macrocrystalline structures are broken down to nanocrystalline structures, but original integrity of the material is retained [10].

On the other hand "Bottom-Up" technique is used to build something from basic materials, for example, assembling materials from the atoms/molecules up, and, therefore very

important for nano-fabrication. Examples of this type are self assembly of nanomaterials, sol-gel technology, physical and chemical vapour deposition (PVD, CVD), epitaxial growth, laser ablation, etc [10].

Synthesis of nanomaterials is based on following strategies:

- Liquid-phase synthesis

- Gas-phase synthesis

- Vapour-phase synthesis

Liquid-phase synthesis

Under Liquid-phase synthesis the techniques used are:

- Co-precipitation
- Sol-gel process
- Micro-emulsions
- Hydrothermal/Solvo-thermal synthesis
- Microwave synthesis
- Sono-chemical synthesis
- Template synthesis

Gas-phased synthesis

- Pulsed Laser Ablation
- Inert Gas Condensation
- Ion Sputtering

Vapour-phased synthesis

- Chemical vapour synthesis
- Spray Pyrolysis
- Laser Pyrolysis/ Photochemical synthesis

Nanostructured materials can have significantly different properties, depending on the chosen fabrication route. Each method offers some advantages over other techniques while suffering limitation from others.

1.5   Objective of Study

Objective of this project is focused on the following steps:

- Preparation of ZnO nanoparticles by wet chemical method. Zinc acetate dehydrate and ethanol are the precursors materials here.
- Characterize the crystal structure and phase using the XRD diffraction pattern.
- Characterize the surface morphology by SEM
- Determination of particle size using TEM
- Detect the various functional groups in molecules of synthesized nanomaterials by FTIR spectroscopy analysis
- Study the optical properties using UV-vis, PL spectroscopy
- Study of Thermal property using TGA
- Study of Transition temperature using DSC
- Study of I-V characteristics and density of state using STM
- Determination of Thermal conductivity and Resistivity using probe technique

Chapter 2

Literature Survey

2.1 Crystal structure of ZnO

Zinc Oxide (ZnO) is a strategically important semiconducting material which potentially has wide application in wireless communications, optoelectronics, including ultraviolet (UV), diode lasers and sensors and MEMS technology [3].

Zinc oxide is an inorganic white powder compound that is insoluble in water, which is widely used as an additive in numerous materials and products including plastic, ceramic glass, cement, paints, batteries and first aid tapes. It occurs naturally as the mineral zincite but most zinc oxide is produced synthetically. In material science zinc oxide is a wide band-gap of 3.37 eV [2, 11, 53, 56, 60] at room temperature and is a semiconductor of the II-VI semiconductor group.

Most of the II-VI binary compound semiconductors crystallize in either cubic zinc blende or hexagonal wurtzite (Wz) structure where each anion is surrounded by four cations at the corners of a tetrahedron and vice versa and it belongs to the space group of *P63mc (186).*

The crystal structure shared by ZnO are wurtzite (B4), zinc blende (B3), and rock salt (or Rochelle salt (B1) [11,12,15].

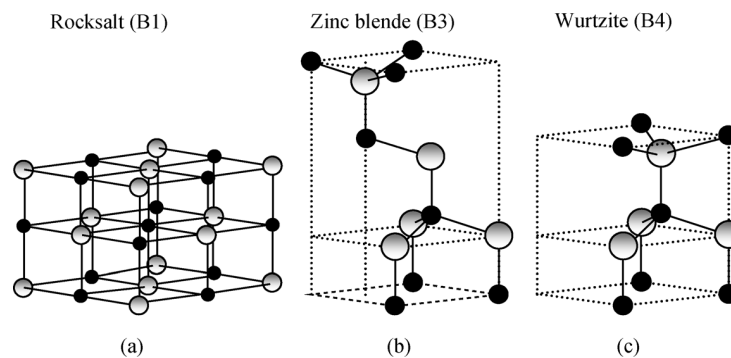Rocksalt (B1) Zinc blende (B3) Wurtzite (B4)

(a) (b) (c)

Fig. 2.1: Stick and ball representation of ZnO structure [14]

It has a stable wurtzite structure [11]. In an ideal wurtzite, with a hexagonal closed packed lattice type has lattice parameters a= 0.325 nm, b= 0.3249 nm and c = 0.521 nm, in the ratio of c / a = 1.602 [12, 58]. The figure below shows the schematic representation of a wurtzite ZnO structure with lattice constants a in the basel plane and c in the basel direction.
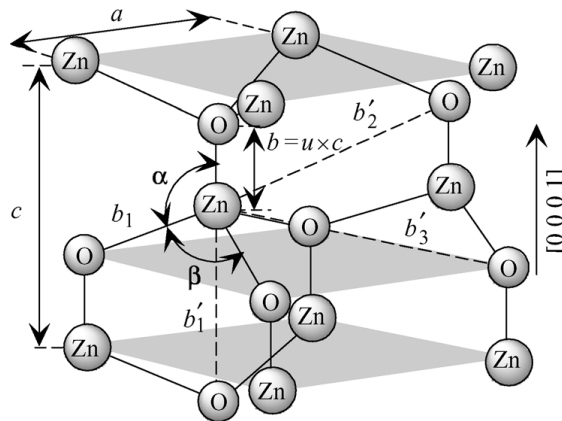

Fig. 2.2: wurtzite ZnO structure with lattice constants a, c and u which is represented as bond length or the nearest-neighbour distance b divided by c (0.375 in ideal crystal), α and β (109.47° in ideal crystal) bond angles and three types of second-nearest-neighbour b_1', b_2', b_3' [14].

It is characterize by two interconnecting sub lattices of Zn^{2+} and O^{2-} where each anion is surrounded by four cations at the corner of a tetrahedron with a typical sp^3 covalent bonding. ZnO has a large free exciton binding energy as 60 meV [1, 3,12, 58] for more efficient optical emission and detection at room temperature and which will strongly prompt the applications of UV laser in the field of benthal detection, communication and optical memory with magnitude enhancement with performance. Much effort has been devoted to tailor the morphology and size to optimize the optical properties. As a result various ZnO nanostructures including nanowires, nanotubes, nanobelts, nanoflowers, nanospheres have been obtained [13].

Moreover, the melting point of ZnO is 1975℃ which determines its high thermal and chemical stability. This kind of tetrahedral coordination in ZnO will form a noncentral symmetric structure with polar symmetry along the hexagonal axis. The root cause for the

natural N-type nature of ZnO is due to the sensitiveness of ZnO lattice constants to the presence of structural point defects (vacancies and interstitials) and extended defects (threading/planar dislocations) that are commonly found in ZnO resulting in a non-stoichiometric compound Zn_{1+d} O with an excess zinc [15]. These excess zinc atoms have the tendency to function as donor interstitials that give its natural N-type conductivity. The cause of the commonly observed unintentional n-type conductivity in as-grown ZnO is still under debate.

Obtaining p-type doping in ZnO has proved to be a very difficult task [1]. One reason is that ZnO has a tendency toward n-type conductivity. Another reason is that the defects, which we now know are not responsible for n-type conductivity, do play a role as compensating centers in p-type doping. A third reason is the fact that there are very few candidate shallow acceptors in ZnO. Column-IA elements (Li, Na, K) on the Zn site are either deep acceptors or are also stable as interstitial donors that compensate p-type conductivity [1]. Column-IB elements (Cu, Ag, Au) are deep acceptors and do not contribute to p-type conductivity. And because O is a highly electronegative first-row element only N is likely to result in a shallow acceptor level in ZnO. The other column-V elements (P, As, Sb) substituting on O sites are all deep acceptors.

In ionic form, the excess zinc exist as Zn+ interstitials that are mobile and they tend to occupy special interstitial sites with Miller index (⅓, ⅔, 0.875) as shown in Figure.2.3
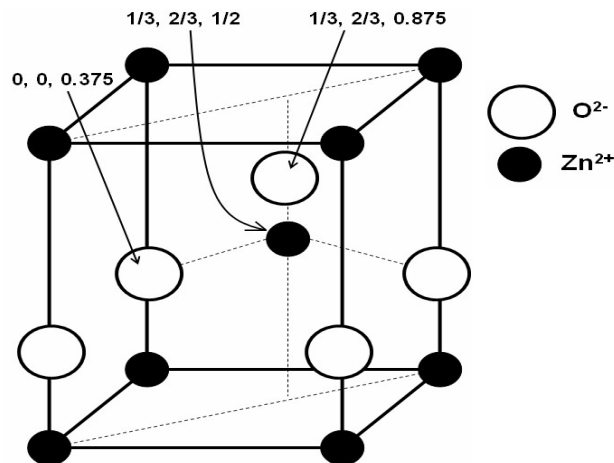

Fig.2.3: ZnO unit cell with ionic positions of Zinc and Oxygen atoms [15]

2.2 Properties of ZnO

As far as properties of ZnO is concerned one can divide them mainly into Chemical properties and Physical properties which are further sub-divided into Mechanical properties, Electrical properties and optoelectronic properties.

2.2.1 Chemical Properties [8]

ZnO possess following chemical properties:

- It occurs as the mineral zincite or as white powder known as zinc white. It is generally orange or red in colour due to manganese impurity.
- It is thermochromic, changing from white to yellow colour when heated and reverting to white colour. This change in colour is caused by a very small loss of oxygen at high temperatures.
- It is amphoteric oxide nearly insoluble in water but it is soluble in most acids and alkalis. With acids it forms compounds like zinc sulphate while with acids it forms zincates.
- On exposed to air it absorbs both water vapour and carbon dioxide. This forms zinc carbonate.

2.2.2 Physical Properties [16]

ZnO possess following physical properties:

Property	Value
Lattice parameters at 300 K	
a	0.325 nm
c	0.521 nm
a / c	1.602 (for ideal hexagonal structure)
u	0.345
Molecular weight	81.38
Density	5.606 g/cm^3
Stable phase at 300 K	Wurtzite
Melting point	1975 ℃

Thermal conductivity	0.6
Linear Expansion coefficient	a_0: 6.5× 10^{-6}, c_0: 3.0× 10^{-6}
Static Dielectric constant	8.656
Refractive Index	2.008
Energy gap	3.37 eV (direct)
Intrinsic carrier concentration	$<10^{-6}\ cm^{-3}$(max n-type doping) $>10^{20}$ cm^{-3} electrons; max p-type doping$<10^{17}$ cm^{-3} holes
Exciton Binding Energy	60 meV
Electron Effective mass	0.24
Electron Hall mobility at 300 K for low n-type conductivity	200 cm^2/Vs
Hall effective mass	0.59
Hole Hall mobility at 300 K for low p-type conductivity	5-50 cm^2/Vs

Table 1: Physical Properties of wurtzite ZnO

2.2.3 Mechanical Properties

Mechanical properties of ZnO including tensile modulus (from tension), bending modulus (from buckling), elasticity and fracture are of critical relevance [17]. ZnO is a relatively soft material with approximate hardness just 4.5. Both tensile modulus and bending modulus were found to increase as nanowire diameter decreased from 80 to 20 nm. The majority of the reported studies focused only on the elastic properties (i.e Young's Modulus).

2.2.4 Electrical Properties

In case of ZnO nanostructure, the surface defects (grain boundary, surface absorbed oxygen and unsaturated dangling bonds) are the most important factors for controlling the electrical conductivity [18]. Doped ZnO is a well-known transparent conductor [38]. The electrical conductivity in ZnO nanomaterials is also an interesting but controversial topic; two different hypotheses are reported as a cause of n-type conductivity in ZnO. Majority of

reports illustrate that the intrinsic defect states like oxygen vacancies or zinc interstitials are responsible for n-type conductivity in ZnO [1, 18]. Though, few other researchers think quite contrary to the hypothesis and believe that intrinsic defects are deep level traps and cannot contribute in conduction.

2.2.5 Magnetic Properties

The perfect crystalline nature along with a defect ridden surface controls the magnetic properties of ZnO nanowire. Magnetic measurements illustrate the ferromagnetic nature of submicron sized zinc oxide (ZnO) arising due to singly charged oxygen vacancies [18]. Nanowires show diamagnetic behavior when annealed at higher temperature in oxygen while argon annealing does not affect the magnetic behaviour [37]. It has been found that ZnO is a promising host material for ferromagnetic doping [12]. Ab initio calculations do predict ferromagnetism in n-type ZnO doped with most transition metalions, including Co and Cr, but predict no ferromagnetism for Mn-doped ZnO. This is consistent with experimental results where ferromagnetism is not observed in Mn-doped ZnO that is n-type due to group III impurities [16, 18].

2.2.6 Optoelectronic Properties

The optical properties of ZnO were characterized by photoluminescence (PL). It has rapidly emerged as a promising optoelectronic material due to its large band gap of 3.37 eV at room temperature, low power threshold for optical pumping and highly efficient UV emission resulting from a large exciton binding energy of 60 meV [1, 3, 12, 19, 20]. The process of optical absorption and emission have been influenced by bound excitons which are extrinsic transition related to dopants or defects thereby usually responsible for creating discrete electronic states in the band gap. Exciton which is a bound system do not requires traps to localize carriers and recombines with high efficiency. The optoelectronic properties of ZnO nanostructures depend strongly on their morphology, crystalline structure, defect and impurity contents [21]. The optoelectronic properties of the nanostructures and the effect of air annealing are further studied by measuring the PL spectra of the samples at room temperature. A broad and intense emission spreading from 450 to 650 nm along with a less intense band at around 385 nm can be seen from the spectra. The 385 nm band is attributed to the band edge excitonic luminescence of ZnO, the broad band in the visible region is generally believed to be associated with intrinsic defects in nominally undoped ZnO [22].

The broad emission near 520 nm in ZnO is often referred as the green emission, while other broad emission at around 580 nm is referred as yellow emission.

2.2.7 Optical Band Gap

An accurate knowledge about the band structure of a semiconductor is quite critical for exploring its applications and even improving the performance. Since both conduction and valence bands contribute significantly to the energy range where the optical excitations fall in, it is impossible to give a detailed interpretation of optical reflectance without at least a semi quantitative band-structure calculation first.

Zinc oxide has a direct and wide band gap (3.37 eV) [11, 12,] as shown in the figure below. It has also a large exciton binding energy of 60 meV and an exciton bohr radius $a_B = 20 \, A^{\circ}$ [22].

(a)   (b)
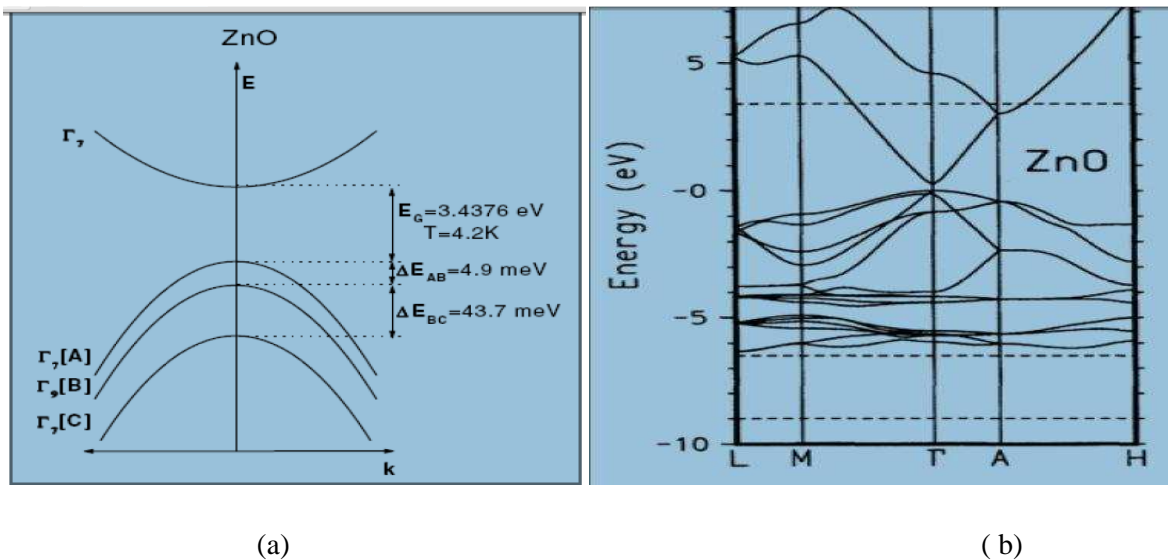
Fig. 2.2.7.1: (a) Band structure and symmetries of hexagonal ZnO. The splitting into three valence bands (A, B, C) is caused by crystal field and spin-orbit splitting (b) The LDA band structure of bulk wurtzite ZnO calculated using a standard pseudopotentials [15,23]

Band-gap engineering of ZnO can be achieved by alloying with MgO or CdO. Adding Mg to ZnO increases the band gap, whereas Cd decreases the band gap, similar to the effects of Al and In in GaN [1].

The band gap of ZnO as calculated by local density approximation (LDA) is found to be 3.77ev which mostly accounts for the Zn 3d electrons. The ZnO having direct band gap is very well indicated by the valence band maxima and lowest conduction band minima both

occurring at the same G point of k=0.Zn 3d levels are indicated by bottom ten bands (occurring around 9ev) and O 2p bonding states are highlighted by next six bands from -5eV to 0 eV. The empty Zn 3s levels signified by first two conduction band states are mainly Zn localized. Crystallization of ZnO mostly favourable in wurtzite symmetry and crystal field splitting as well as spin orbit interaction results in three states say A, B &C.

CHAPTER-3

MATERIALS AND METHODES

3.1 EXPERIMENTAL

The precursors used in the synthesis of ZnO nano particles by wet chemical method are Zinc acetate dihydrate ((CH_3COO)$_2$ Zn 2H$_2$O) with molecular weight of 219.50 gm and ethanol (CH_3CH_2OH) having a molecular weight of 46.08 gm. Ethanol takes care for the homogeneity and PH value of the solution and helps to make a stoichiometric solution to get Zinc oxide nanoparticles [24].

Steps involved in the synthesis of ZnO nanoparticles are as:

- Firstly in a 50 ml beaker take 500 mg of Zn acetate and dissolve it in a 20ml of Ethanol along with continuous stirring. This will result in a homogenous solution.

- After this transfer the above prepared homogenous solution in a crucible or watch-glass and add 2-3 drops of Ethyl Acetate ($CH_3COOCH_2CH_3$) with constant stirring.

- Heat the above prepared solution at 40℃ to evaporate the solution. This will result in a white powder.

- The white powder obtained is subjected to calcinations at three different temperatures 450℃, 700℃, 900℃ for 3 hours.

The growth of ZnO from zinc acetate dihydrate precursor using wet chemical process generally undergoes four stages, such as solvation, hydrolysis, polymerization and transformation into ZnO. The zinc acetate dihydrate precursor was first solvated in ethanol, and then hydrolyzed, regarded as removal of the intercalated acetate ions. Ethanol has smaller size and a more active – OH. Ethanol can react more easily to form a polymer precursor with a higher polymerization degree. These zinc hydroxide splits into Zn cation and OH- anion according to reactions (Eq. (1)) and followed by polymerization of hydroxyl complex to form "Zn–O–Zn" bridges and finally transformed into ZnO (Eq. (2)) [25].

$$Zn\,(OAc)_2 \implies 2Zn^{2+} + 2(OAc)^- \qquad (1)$$

$$Zn^{2+} + 2OH^- \implies Zn\,(OH)_2 \implies ZnO + H_2O \qquad (2)$$
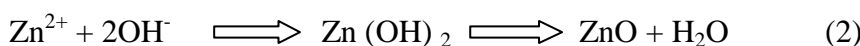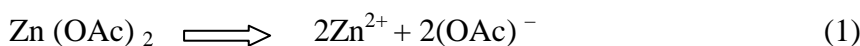
The calcinated powders are studied using different characterisation techniques. Confirmation of pure ZnO phase is verified by XRD analysis. The shape and morphology of particles are studied by SEM pictures obtained. Whether the particles have attended the nano range is studied by taking the TEM pictures of sample which gives the sharp peaks in XRD analysis. Optical properties were studied by PL and electrical properties using STM. Resistance can be measured using High resistance meter.

3.2 CHARACTERISATION TECHNIQUES

In order to investigate various properties of the prepared sample, it has to goes under a number of characterisation techniques. The result gives the information about the different optical, electrical as structural properties of sample.

3.2.1 Structural Characterisation

Structural characterisation is done to get exact information about the crystal structure, surface morphology, particle size etc using XRD (X-ray Diffraction), SEM (Scanning electron microscope), TEM (Transmission electron microscope).

3.2.1.1 XRD

Up to 1895 the study of matter at the atomic level was a difficult task but the discovery of electromagnetic radiation with 1 Å (10-10 m) wavelength, appearing at the region between gamma-rays and ultraviolet, makes it possible. As the atomic distance in matter is comparable with the wavelength of X-ray, the phenomenon of diffraction find its way through it and gives many promisable results related to the crystalline structure.

Crystals are regular arrays of atoms, and X-rays can be considered waves of electromagnetic radiation. Atoms scatter X-ray waves, primarily through the atoms' electrons. Just as an ocean wave striking a lighthouse produces secondary circular waves emanating from the lighthouse, so pan X-ray striking an electron produces secondary spherical waves emanating from the electron. This phenomenon is known as elastic scattering, and the electron (or lighthouse) is known as the scatterer. A regular array of scatterers produces a regular array of spherical waves. Although these waves cancel one another out in most directions through destructive interference, they add constructively in a few specific directions, determined by Bragg's law.

$$2d \sin \theta = n \lambda$$

Where *n* is an integer 1, 2, 3….. (Usually equal 1), λ is wavelength in angstroms (1.54 Å for copper), d is interatomic spacing in A°, and θ is the diffraction angle in degrees.

The characteristic of the sample can be determined by plotting the angular positions and intensities of the resultant diffracted peaks of radiation. XRD is used to determine the structure of sample, i.e. how the atoms pack together in the crystalline state and what the interatomic distances and angle are.

Fig. 3.2.1 (a): X-Ray diffraction in accordance with Bragg's law [26]

The figure shows the X-Ray diffractometer Brucker D8 advance available in DTU.

Fig.3.2.1 (b): Photograph of Bruker D8 Advance

The main components of XRD are an X-ray tube, a sample holder, and an X-ray detector. X-rays are generated by in a cathode ray tube by heating a filament to produce electrons,

accelerating the electrons toward a target by applying a voltage, and bombarding the target material with electrons. When electrons have sufficient energy to dislodge inner shell electrons of the target material, characteristic X-ray spectra are produced. These spectra consist of several components, the most common being K_α and K_β. K_α consists, in part, of $K_{\alpha 1}$ and $K_{\alpha 2}$. $K_{\alpha 1}$ has a slightly shorter wavelength and twice the intensity as $K_{\alpha 2}$. The specific wavelengths are characteristic of the target material (Cu, Fe, Mo, Cr). Filtering, by foils or crystal monochrometers, is required to produce monochromatic X-rays needed for diffraction. $K_{\alpha 1}$ and $K_{\alpha 2}$ is sufficiently close in wavelength such that a weighted average of the two is used. Copper is the most common target material for single-crystal diffraction, with Cu K_α radiation = 1.5418Å [27]. These X-rays are collimated and directed onto the sample. As the sample and detector are rotated, the intensity of the reflected X-rays is recorded. When the geometry of the incident X-rays impinging the sample satisfies the Bragg Equation, constructive interference occurs and a peak in intensity occurs. A detector records and processes this X-ray signal and converts the signal to a count rate which is then output to a device such as a printer or computer monitor.

The geometry of an X-ray diffractometer is such that the sample rotates in the path of the collimated X-ray beam at an angle θ while the X-ray detector is mounted on an arm to collect the diffracted X-rays and rotates at an angle of 2θ. The instrument used to maintain the angle and rotate the sample is termed a goniometer. For typical powder patterns, data is collected at 2θ from ~5° to 70°, angles that are preset in the X-ray scan.

3.2.1.2 Scanning Electron Microscope SEM

A scanning electron microscope (SEM) is a type of electron microscope that produces images of a sample by scanning it with a focused beam of electrons. The electrons interact with atoms in the sample, producing various signals that can be detected and that contain information about the sample's surface topography and composition. The signals that derive from electron reveal information about the sample including external morphology (texture), chemical composition, and crystalline structure and orientation of materials making up the sample. In most applications, data are collected over a selected area of the surface of the sample, and a 2-dimensional image is generated that displays spatial variations in these properties. The electron beam is generally scanned in a raster scan pattern, and the beam's position is combined with the detected signal to produce an image.

A typical SEM consists of electron gun, electron lenses, sample stage, detector for all signals of interest, display/data output devices. In most applications, data are collected over a selected area of the surface of the sample, and a 2-dimensional image is generated that displays spatial variations in these properties. Areas ranging from approximately 1 cm to 5 microns in width can be imaged in a scanning mode using conventional SEM techniques (magnification ranging from 20X to approximately 30,000X, spatial resolution of 50 to 100 nm) [28]. The SEM is also capable of performing analyses of selected point locations on the sample; this approach is especially useful in qualitatively or semi-quantitatively determining chemical compositions (using EDS), crystalline structure, and crystal orientations (using EBSD). The design and function of the SEM is very similar to the EPMA and considerable overlap in capabilities exists between the two instruments.

The figure shows a typical SEM:
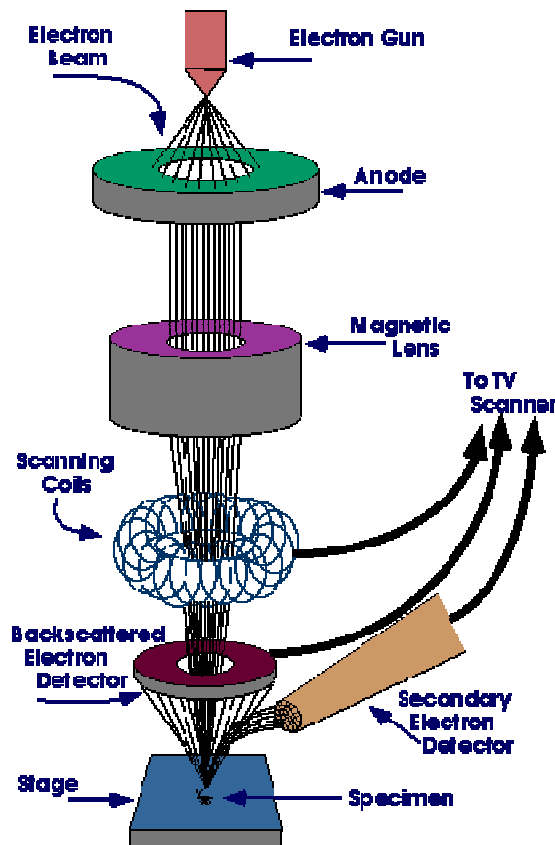
Fig.3.2.1 (c): Schematic SEM [29]

The SEM is an instrument that produces a largely magnified image by using electrons instead of light to form an image. A beam of electrons is produced at the top of the microscope by an electron gun. The electron beam follows a vertical path through the microscope, which is held within a vacuum. The beam travels through electromagnetic

fields and lenses, which focus the beam down toward the sample. Once the beam hits the sample, electrons and X-rays are ejected from the sample.

Detectors collect these X-rays, backscattered electrons, and secondary electrons and convert them into a signal that is sent to a screen similar to a television screen. This produces the final image. Because the SEM utilizes vacuum conditions and uses electrons to form an image, special preparations must be done to the sample. All water must be removed from the samples because the water would vaporize in the vacuum. All metals are conductive and require no preparation before being used. All non-metals need to be made conductive by covering the sample with a thin layer of conductive material. This is done by using a device called a "sputter coater." The sputter coater uses an electric field and argon gas. The sample is placed in a small chamber that is at a vacuum. Argon gas and an electric field cause an electron to be removed from the argon, making the atoms positively charged. The argon ions then become attracted to a negatively charged gold foil. The argon ions knock gold atoms from the surface of the gold foil. These gold atoms fall and settle onto the surface of the sample producing a thin gold coating. The figure shows the Hitachi-s-3700 N available in DTU.

Fig. 3.2.1 (d) Hitachi-s-3700 N

3.2.1.3 Transmission Electron Microscopy (TEM)

Transmission electron microscopy (TEM) is a microscopy technique whereby a beam of electrons instead of light is transmitted through an ultra-thin specimen, interacting with the specimen as it passes through. An image is formed from the interaction of the electrons transmitted through the specimen; the image is magnified and focused onto an imaging device, such as a fluorescent screen, on a layer of photographic film, or to be detected by a sensor such as a CCD camera.

A TEM is composed of several components, which include a vacuum system in which the electron travel, an electron emission source for generation of the electron stream, a series of electromagnetic lenses, as well as electrostatic plates. The latter two allow the operator to guide and manipulate the beam as required. Also required is a device to allow the insertion into, motion within, and removal of specimens from the beam path. Imaging devices are subsequently used to create an image from the electrons that exit the system.

Theoretically, the maximum resolution, d, that one can obtain with a light microscope has been limited by the wavelength of the photons that are being used to probe the sample, λ and the numerical aperture of the system, NA [31].

$$d = \frac{\lambda}{2n \sin \alpha} \approx \frac{\lambda}{2\,\mathrm{NA}}$$

Early twentieth century scientist theorised ways of getting around the limitations of the relatively large wavelength of visible light (wavelengths of 400–700 nanometers) by using electrons. Like all matter, electrons have both wave and particle properties (as theorized by Louis-Victor de Broglie), and their wave-like properties mean that a beam of electrons can be made to behave like a beam of electromagnetic radiation. The wavelength of electrons is related to their kinetic energy via the de Broglie equation. An additional correction must be made to account for relativistic effects, as in a TEM electron's velocity approaches the speed of light, c.

$$\lambda_e \approx \frac{h}{\sqrt{2m_0 E \left(1 + \frac{E}{2m_0 c^2}\right)}}$$

Where, h is Planck's constant, m_0 is the rest mass of an electron and E is the energy of the accelerated electron. Electrons are usually generated in an electron

microscope by a process known as thermionic emission from a filament, usually tungsten, in the same manner as a light bulb, or alternatively by field electron emission. The electrons are then accelerated by an electric potential (measured in volts) and focused by electrostatic and electromagnetic lenses onto the sample. The transmitted beam contains information about electron density, phase and periodicity; this beam is used to form an image.
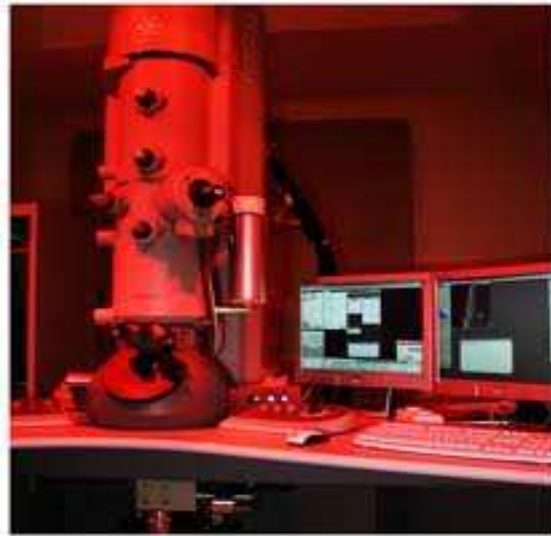
The figure shows the TEM used for characterisation

Fig.3.2.1 (e) Photograph of TEM

Figure illustrates the internal construction of TEM:
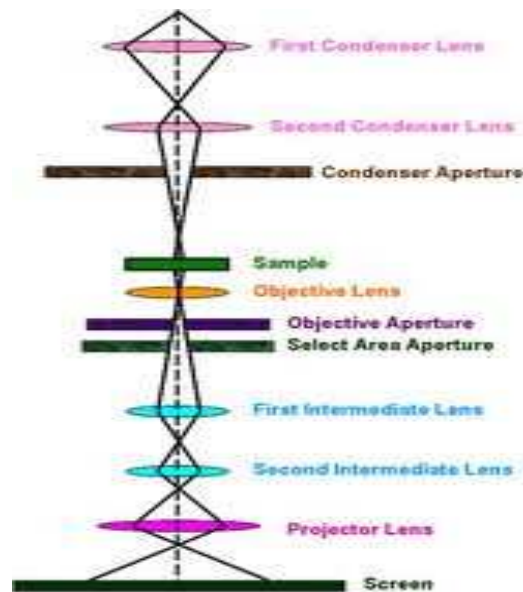
Fig.3.2.1 (f) Internal Structure of TEM [30]

3.2.2 Optical Characterisation

As we know zinc oxide has wide range of application in the field of optoelectronics devices on putting the sample to following characterisation techniques gives information related to optical properties.

- UV-visible spectroscopy
- Fourier Transform infrared spectroscopy
- Photoluminescence

3.2.2.1 Fourier Transform infrared (FTIR)

In the region of longer wavelength or low frequency the identification of different types of chemicals is possible by this technique of infrared spectroscopy and the instrument requires for its execution is Fourier transform infrared (FTIR) spectrometer. The spectroscopy merely based on the fact that molecules absorb specific frequencies that are characteristic of their structure termed as resonant frequencies, i.e. the frequency of the absorbed radiation matches the frequency of the bond or group that vibrates. And the detection of energy is done on the basis of shape of the molecular potential energy surfaces, the masses of the atoms, and the associated vibronic coupling energy is done on the basis of shape of the molecular potential energy surfaces, the masses of the atoms, and the associated vibronic coupling.

As each different material is a unique combination of atoms, no two compounds produce the exact same infrared spectrum. Therefore, infrared spectroscopy can result in a positive identification (qualitative analysis) of every different kind of material. In addition, the size of the peaks in the spectrum is a direct indication of the amount of material present. In infrared spectroscopy, IR radiation is passed through a sample. Some of the infrared radiation is absorbed by the sample and some of it is passed through (transmitted). The resulting spectrum represents the molecular absorption and transmission, creating a molecular fingerprint of the sample. Like a fingerprint no two unique molecular structures produce the same infrared spectrum. This makes infrared spectroscopy useful for several types of analysis.

The figure shows the FTIR available in DTU:

Fig.3.2.2 (a): Photograph of Nicolet-380 FTIR

The goal of any absorption spectroscopy (FTIR, ultraviolet-visible ("UV-Vis") spectroscopy, etc.) is to measure how well a sample absorbs light at each wavelength. The most straightforward way to do this, the "dispersive spectroscopy" technique, is to shine a monochromatic light beam at a sample, measure how much of the light is absorbed, and repeat for each different wavelength.
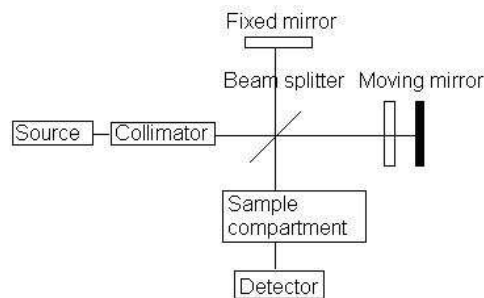
The figure shows the components of FTIR:

Fig.3.2.2 (b): Internal Structure of FTIR [33]

FTIR analysis can give not only qualitative (identification) analysis of materials, but with relevant standards, can be used for quantitative (amount) analysis. FTIR can be used to analyze samples up to ~11 millimetres in diameter, and either measure in bulk or the top ~1 micrometer layer.

3.2.2.2 Photoluminescence

Photoluminescence (abbreviated as PL) describes the phenomenon of light emission from any form of matter after the absorption of photons (electromagnetic radiation). Photoluminescence (PL) is the spontaneous emission of light from a material under optical excitation. Features of the emission spectrum can be used to identify surface, interface, and impurity levels and to gauge alloy disorder and interface roughness. The intensity of the PL signal provides information on the quality of surfaces and interfaces [34].

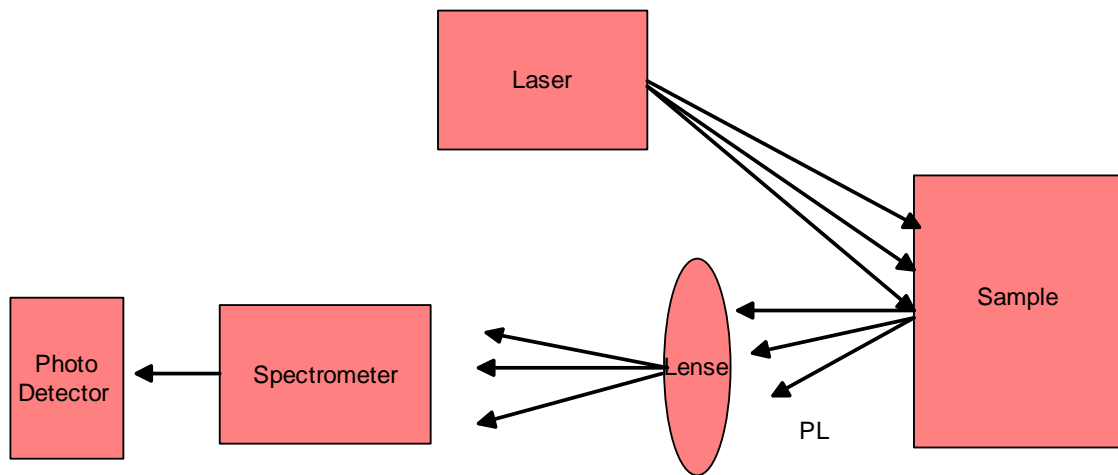Figure below shows the typical experimental set up for PL measurement.

Fig.3.2.2 (c) Set up for PL [34]

In a typical PL experiment, a semiconductor is excited with a light-source that provides photons with energy larger than the band-gap energy. The incoming light excites a polarization that can be described with the semiconductor Bloch equations. Once the photons are absorbed, electrons and holes are formed with finite momenta k in the conduction and valence bands, respectively. The excitations then undergo energy and momentum relaxation towards the band gap minimum. Typical mechanisms are Coulomb scattering and the interaction with phonons. Finally, the electrons recombine with holes under emission of photons.

Ideal, defect-free semiconductors are many-body systems where the interactions of charge-carriers and lattice vibrations have to be considered in addition to the light-matter coupling. In general, the PL properties are also extremely sensitive to internal electric fields and to the dielectric environment (such as in photonic crystals) which impose further degrees of complexity.

Figure shows the PL instrument:

Fig.3.2.2 (d) Photograph of PL Instrument

3.2.3.1 HIGH RESISTANCE METER/ ELECTROMETR

An Electrometer is an electrical instrument for measuring electric charge or electrical potential difference. There are many different types, ranging from historical handmade mechanical instruments to high-precision electronic devices. In order to study electrical properties (resistance) of ZnO nano-particles electrometer/ high resistance meter is used.

Modern electrometer is a highly sensitive electronic voltmeter whose input impedance is so high that the current flowing into it can be considered, for most practical purposes, to be zero. The actual value of input resistance for modern electronic electrometers is around $10^{14}\Omega$, compared to around $10^{10}\Omega$ for nano-voltmeters.

Here we measured resistance with variation of temperature. The photograph below shows the Electrometer 6517A available in DTU.

Fig.3.2.3 (a) Photograph of 6517A Electrometer

3.2.3.2 STM

The development of the family of scanning probe microscopes starts with the original invention of the STM in 1981.Gerd Binnig and Heinrich Rohrer developed the first working STM while working at IBM Zurich Research Laboratories in Switzerland. This instrument would later win Binnig and Rohrer the Nobel Prize in physics in 1986 [35]. A scanning tunnelling microscope (STM) is a non-optical microscope that works by scanning an electrical probe tip over the surface of a sample at a constant spacing. This allows for a 3D picture of the surface to be created.

The STM works by scanning a very sharp metal wire tip over a surface. By bringing the tip very close to the surface, and by applying an electrical voltage to the tip or sample, we can image the surface at an extremely small scale – down to resolving individual atoms. The STM sample must conduct electricity for the process to work. For an STM, good resolution is considered to be 0.1 nm lateral resolution and 0.01 nm depth resolution. With this resolution, individual atoms within materials are routinely imaged and manipulated. The STM can be used not only in ultra-high vacuum but also in air, water, and various other liquid or gas ambient, and at temperatures ranging from near zero Kelvin to a few hundred degrees Celsius.

In addition to scanning across the sample, information on the electronic structure at a given location in the sample can be obtained by sweeping voltage and measuring current at a specific location. This type of measurement is called scanning tunnelling spectroscopy (STS) and typically results in a plot of the local density of states as a function of energy within the sample.

Working Principle of STM

The STM is based on several principles. One is the quantum mechanical effect of tunnelling. It is this effect that allows us to "see" the surface. Another principle is the piezoelectric effect. It is this effect that allows us to precisely scan the tip with angstrom-level control. Lastly, a feedback loop is required, which monitors the tunnelling current and coordinates the current and the positioning of the tip.

Modes of Operation

First, a voltage bias is applied and the tip is brought close to the sample by coarse sample-to-tip control, which is turned off when the tip and sample are sufficiently close. At close range, fine control of the tip in all three dimensions when near the sample is typically piezoelectric, maintaining tip-sample separation W typically in the 4-7 Å (0.4-0.7 nm) range, which is the equilibrium position between attractive ($3<W<10$Å) and repulsive ($W<3$Å) interactions. In this situation, the voltage bias will cause electrons to tunnel between the tip and sample, creating a current that can be measured. Once tunnelling is established, the tip's bias and position with respect to the sample can be varied (with the details of this variation depending on the experiment) and data are obtained from the resulting changes in current.

If the tip is moved across the sample in the x-y plane, the changes in surface height and density of states cause changes in current. These changes are mapped in images. This change in current with respect to position can be measured itself, or the height, z, of the tip corresponding to a constant current can be measured. These two modes are called constant height mode and constant current mode, respectively.

In constant current mode, feedback electronics adjust the height by a voltage to the piezoelectric height control mechanism. This leads to a height variation and thus the image comes from the tip topography across the sample and gives a constant charge density surface; this means contrast on the image is due to variations in charge density. In constant height mode, the voltage and height are both held constant while the current changes to keep the voltage from changing; this leads to an image made of current changes over the surface, which can be related to charge density. The benefit to using a constant height mode is that it is faster, as the piezoelectric movements require more time to register the height change in constant current mode than the current change in constant height mode.

The figure below shows the STM along with its components:

Fig.3.2.3 (b) Components of STM [8]

The photograph shows the STM available in DTU.

Fig.3.2.3 (c) Photograph of STM

CHAPTER-4

CHARACTERISATION TECHNIQUES

In order to investigate various properties of the prepared sample, it has to goes under a number of characterisation techniques. The result gives the information about the different optical, electrical as structural properties of sample.

4.1 Structural Characterisation

Structural characterisation is done to get exact information about the crystal structure, surface morphology, particle size etc the following techniques are available

- XRD (X-ray Diffraction)
- SEM (Scanning electron microscope)
- TEM (Transmission electron microscope)

4.2 Optical Characterisation

As we know zinc oxide has wide range of application in the field of optoelectronics devices on putting the sample to following characterisation techniques gives information related to optical properties.

- UV-visible spectroscopy
- Fourier Transform infrared spectroscopy
- Photoluminescence

4.3 Electrical Properties Analysis

- LCR meter to measure Resistance
- STM (Scanning Tunnelling Microscope
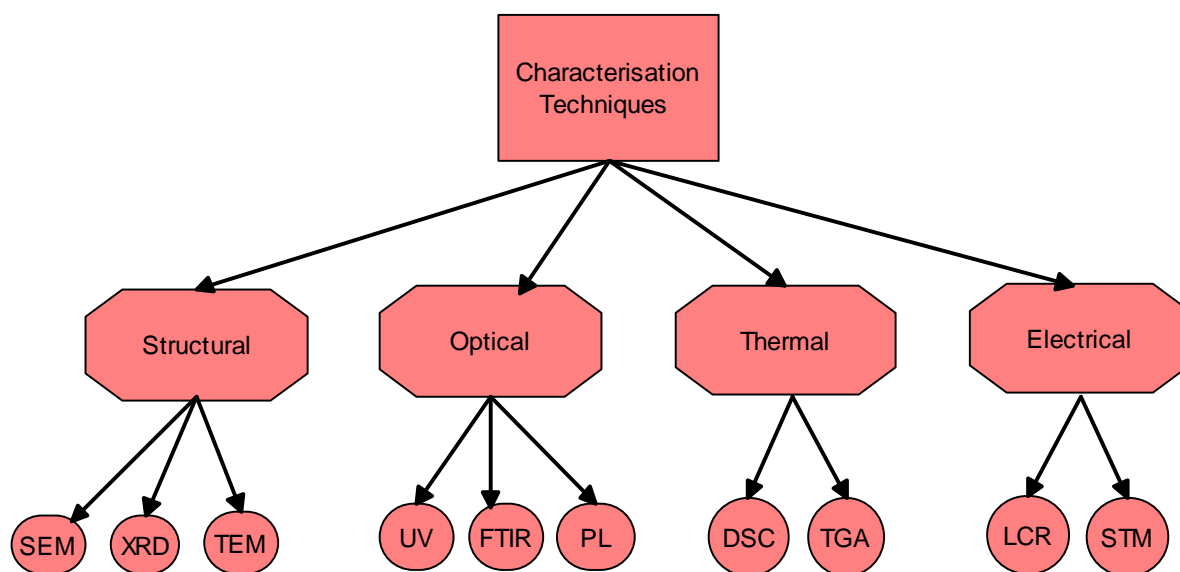
Fig. 4.1: Characterization Methods

4.1.1 XRD

Up to 1895 the study of matter at the atomic level was a difficult task but the discovery of electromagnetic radiation with 1 Å (10-10 m) wavelength, appearing at the region between gamma-rays and ultraviolet, makes it possible. As the atomic distance in matter is comparable with the wavelength of X-ray, the phenomenon of diffraction find its way through it and gives many promisable results related to the crystalline structure.

Crystals are regular arrays of atoms, and X-rays can be considered waves of electromagnetic radiation. Atoms scatter X-ray waves, primarily through the atoms' electrons. Just as an ocean wave striking a lighthouse produces secondary circular waves emanating from the lighthouse, so pan X-ray striking an electron produces secondary spherical waves emanating from the electron. This phenomenon is known as elastic scattering, and the electron (or lighthouse) is known as the scatterer. A regular array of scatterers produces a regular array of spherical waves. Although these waves cancel one another out in most directions through destructive interference, they add constructively in a few specific directions, determined by Bragg's law.

$$2d \sin\theta = n\,\lambda$$

Where *n* is an integer 1, 2, 3….. (Usually equal 1), λ is wavelength in angstroms (1.54 Å for copper), d is interatomic spacing in A°, and θ is the diffraction angle in degrees.

The characteristic of the sample can be determined by plotting the angular positions and intensities of the resultant diffracted peaks of radiation. XRD is used to determine the structure of sample, i.e. how the atoms pack together in the crystalline state and what the interatomic distances and angle are.
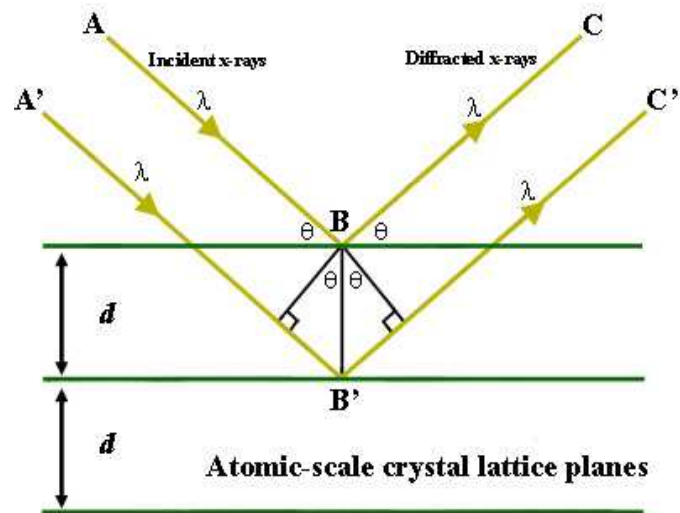

Fig. 4.2: X-Ray diffraction in accordance with Bragg's law [26]

The figure below shows the X-Ray diffractometer Brucker D8 advance available in DTU.

Fig.4.3: Bruker D8 Advance

The main components of XRD are an X-ray tube, a sample holder, and an X-ray detector. X-rays are generated by in a cathode ray tube by heating a filament to produce electrons, accelerating the electrons toward a target by applying a voltage, and bombarding the target material with electrons. When electrons have sufficient energy to dislodge inner shell electrons of the target material, characteristic X-ray spectra are produced. These spectra consist of several components, the most common being K_α and K_β. K_α consists, in part, of

$K_{\alpha 1}$ and $K_{\alpha 2}$. $K_{\alpha 1}$ has a slightly shorter wavelength and twice the intensity as $K_{\alpha 2}$. The specific wavelengths are characteristic of the target material (Cu, Fe, Mo, Cr). Filtering, by foils or crystal monochrometers, is required to produce monochromatic X-rays needed for diffraction. $K_{\alpha 1}$ and $K_{\alpha 2}$ is sufficiently close in wavelength such that a weighted average of the two is used. Copper is the most common target material for single-crystal diffraction, with Cu K_{α} radiation = 1.5418Å [27]. These X-rays are collimated and directed onto the sample. As the sample and detector are rotated, the intensity of the reflected X-rays is recorded. When the geometry of the incident X-rays impinging the sample satisfies the Bragg Equation, constructive interference occurs and a peak in intensity occurs. A detector records and processes this X-ray signal and converts the signal to a count rate which is then output to a device such as a printer or computer monitor.

The geometry of an X-ray diffractometer is such that the sample rotates in the path of the collimated X-ray beam at an angle θ while the X-ray detector is mounted on an arm to collect the diffracted X-rays and rotates at an angle of 2θ. The instrument used to maintain the angle and rotate the sample is termed a goniometer. For typical powder patterns, data is collected at 2θ from ~5° to 70°, angles that are preset in the X-ray scan.

4.1.2 SEM

A scanning electron microscope (SEM) is a type of electron microscope that produces images of a sample by scanning it with a focused beam of electrons. The electrons interact with atoms in the sample, producing various signals that can be detected and that contain information about the sample's surface topography and composition. The signals that derive from electron reveal information about the sample including external morphology (texture), chemical composition, and crystalline structure and orientation of materials making up the sample. In most applications, data are collected over a selected area of the surface of the sample, and a 2-dimensional image is generated that displays spatial variations in these properties. The electron beam is generally scanned in a raster scan pattern, and the beam's position is combined with the detected signal to produce an image.
A typical SEM consists of electron gun, electron lenses, sample stage, detector for all signals of interest, display/data output devices. In most applications, data are collected over a selected area of the surface of the sample, and a 2-dimensional image is generated that displays spatial variations in these properties. Areas ranging from approximately 1 cm to 5 microns in width can be imaged in a scanning mode using conventional SEM techniques

(magnification ranging from 20X to approximately 30,000X, spatial resolution of 50 to 100 nm) [28]. The SEM is also capable of performing analyses of selected point locations on the sample; this approach is especially useful in qualitatively or semi-quantitatively determining chemical compositions (using EDS), crystalline structure, and crystal orientations (using EBSD). The design and function of the SEM is very similar to the EPMA and considerable overlap in capabilities exists between the two instruments.

The figure below shows a typical SEM:

Fig.4.4: SEM [29]

The SEM is an instrument that produces a largely magnified image by using electrons instead of light to form an image. A beam of electrons is produced at the top of the microscope by an electron gun. The electron beam follows a vertical path through the microscope, which is held within a vacuum. The beam travels through electromagnetic fields and lenses, which focus the beam down toward the sample. Once the beam hits the sample, electrons and X-rays are ejected from the sample.

Detectors collect these X-rays, backscattered electrons, and secondary electrons and convert them into a signal that is sent to a screen similar to a television screen. This produces the final image. Because the SEM utilizes vacuum conditions and uses electrons to form an image, special preparations must be done to the sample. All water must be removed from the samples because the water would vaporize in the vacuum. All metals are conductive and require no preparation before being used. All non-metals need to be made conductive by covering the sample with a thin layer of conductive material. This is done by using a device called a "sputter coater." The sputter coater uses an electric field and argon gas. The sample is placed in a small chamber that is at a vacuum. Argon gas and an electric field cause an electron to be removed from the argon, making the atoms positively charged. The argon ions then become attracted to a negatively charged gold foil. The argon ions knock gold atoms from the surface of the gold foil. These gold atoms fall and settle onto the surface of the sample producing a thin gold coating. The figure below shows the Hitachi-s-3700 N available in DTU.

Fig. 4.5: Hitachi-s-3700 N

4.1.3 TEM

Electron Microscopes are scientific instruments that use a beam of highly energetic electrons to examine objects on a very fine scale. This examination can yield the information like topography, morphology, composition as well as crystallographic information's. Working principle is exactly as their optical counterparts except that they use a focused beam of electrons instead of light to "image" the specimen and gain information as to its structure and composition. The main use of this technique is to examine the specimen structure, composition or properties in sub-microscopic details so that this microscopy technique is significantly involved in numerous fields.

Transmission electron microscopy (TEM) is a microscopy technique whereby a beam of electrons instead of light is transmitted through an ultra-thin specimen, interacting with the specimen as it passes through. An image is formed from the interaction of the electrons transmitted through the specimen; the image is magnified and focused onto an imaging device, such as a fluorescent screen, on a layer of photographic film, or to be detected by a sensor such as a CCD camera.

TEM's uses electrons as "light source" and their much lower de Broglie wavelength makes it possible to get a resolution of thousand times better than with a light microscope. One can see objects to the order of a few angstroms. At smaller magnifications TEM image contrast is due to absorption of electrons in the material, due to the thickness and composition of the material. The first TEM was built by Max Knoll and Ernst Ruska in 1931, with this group developing the first TEM with resolving power greater than that of light in 1933 and the first commercial TEM in 1939.

A TEM is composed of several components, which include a vacuum system in which the electron travel, an electron emission source for generation of the electron stream, a series of electromagnetic lenses, as well as electrostatic plates. The latter two allow the operator to guide and manipulate the beam as required. Also required is a device to allow the insertion into, motion within, and removal of specimens from the beam path. Imaging devices are subsequently used to create an image from the electrons that exit the system.

Theoretically, the maximum resolution, d, that one can obtain with a light microscope has been limited by the wavelength of the photons that are being used to probe the sample, λ and the numerical aperture of the system, NA [31].

$$d = \frac{\lambda}{2n\sin\alpha} \approx \frac{\lambda}{2\,\mathrm{NA}}$$

Early twentieth century scientist theorised ways of getting around the limitations of the relatively large wavelength of visible light (wavelengths of 400–700 nanometers) by using electrons. Like all matter, electrons have both wave and particle properties (as theorized by Louis-Victor de Broglie), and their wave-like properties mean that a beam of electrons can be made to behave like a beam of electromagnetic radiation. The wavelength of electrons is related to their kinetic energy via the de Broglie equation. An additional correction must be made to account for relativistic effects, as in a TEM electron's velocity approaches the speed of light, *c*.

$$\lambda_e \approx \frac{h}{\sqrt{2m_0 E \left(1 + \frac{E}{2m_0 c^2}\right)}}$$

Where, *h* is Planck's constant, m_0 is the rest mass of an electron and *E* is the energy of the accelerated electron. Electrons are usually generated in an electron microscope by a process known as thermionic emission from a filament, usually tungsten, in the same manner as a light bulb, or alternatively by field electron emission. The electrons are then accelerated by an electric potential (measured in volts) and focused by electrostatic and electromagnetic lenses onto the sample. The transmitted beam contains information about electron density, phase and periodicity; this beam is used to form an image.

The figure below shows the TEM used for characterisation
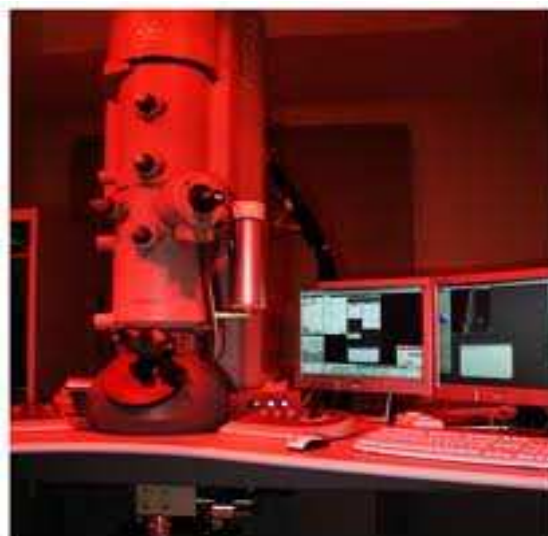
Fig.4.6 TEM

Figure below illustrate the internal construction of TEM:
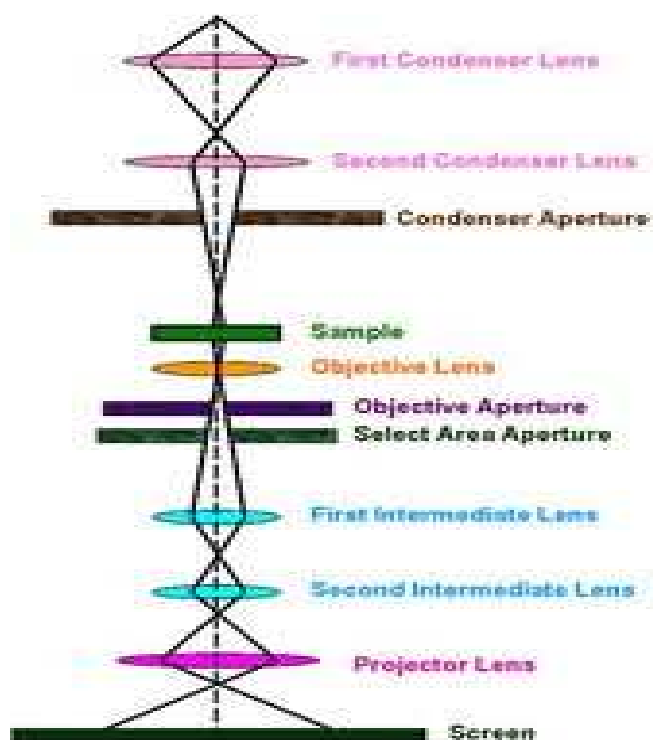
Fig.4.7 Internal Structure of TEM [30]

4.2.1 UV-visible Spectroscopy

Ultraviolet–visible spectroscopy or ultraviolet-visible spectro- photometry (UV-Vis or UV/Vis) refers to absorption spectroscopy or reflectance spectroscopy in the ultraviolet-visible spectral region. This means it uses light in the visible and adjacent (near-UV and near-infrared (NIR)) ranges. The absorption or reflectance in the visible range directly affects the perceived colour of the chemicals involved. In this region of the electromagnetic spectrum, molecules undergo electronic transitions. This technique is complementary to fluorescence spectroscopy, in that fluorescence deals with transitions from the excited state to the ground state, while absorption measures transitions from the ground state to the excited state.

The instrument used in ultraviolet-visible spectroscopy is called a UV/Vis spectrophotometer. It measures the intensity of light passing through a sample (I), and compares it to the intensity of light before it passes through the sample (I_0). The ratio $\frac{I}{I_0}$ is called the transmittance. Absorption may be presented as transmittance (T = I/I_0)

34

or absorbance ($A= \log I_0/I$). Absorbance is directly proportional to the path length, *b*, and the concentration, *c*, of the absorbing species. *Beer's Law* states that

A $= \varepsilon bc$, where ε is a constant of proportionality known as the molar absorbtivity or extinction coefficient, called the absorbtivity in Absorbance units (AU).

If no absorption has occurred, T = 1.0 and *A*= 0. Most spectrometers display absorbance on the vertical axis, and the commonly observed range is from 0 (100% transmittance) to 2 (1% transmittance) [31]. The wavelength of maximum absorbance is a characteristic value, designated as λ_{max}.

A diagram shows the components of a typical spectrometer are shown in the following diagram. The basic parts of a spectrophotometer are a light source, a holder for the sample, a diffraction grating in a mono-chromator or a prism to separate the different wavelengths of light, and a detector.

The ultraviolet (UV) region scanned is normally from 200 to 400 nm, and the visible portion is from 400 to 800 nm.
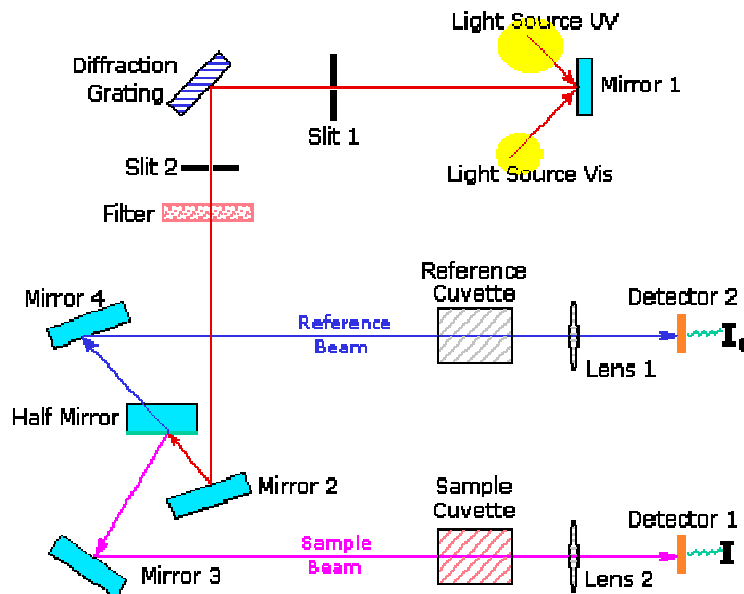
Fig.4.8: UV-visible Spectrometer [32]

The figure below shows the UV 5704 instrument:

Fig.4.9: UV-5704

4.2.2 FTIR

In the region of longer wavelength or low frequency the identification of different types of chemicals is possible by this technique of infrared spectroscopy and the instrument requires for its execution is Fourier transform infrared (FTIR) spectrometer. The spectroscopy merely based on the fact that molecules absorb specific frequencies that are characteristic of their structure termed as resonant frequencies, i.e. the frequency of the absorbed radiation matches the frequency of the bond or group that vibrates. And the detection of energy is done on the basis of shape of the molecular potential energy surfaces, the masses of the atoms, and the associated vibronic coupling energy is done on the basis of shape of the molecular potential energy surfaces, the masses of the atoms, and the associated vibronic coupling.

As each different material is a unique combination of atoms, no two compounds produce the exact same infrared spectrum. Therefore, infrared spectroscopy can result in a positive identification (qualitative analysis) of every different kind of material. In addition, the size of the peaks in the spectrum is a direct indication of the amount of material present. In infrared spectroscopy, IR radiation is passed through a sample. Some of the infrared radiation is absorbed by the sample and some of it is passed through

(transmitted). The resulting spectrum represents the molecular absorption and transmission, creating a molecular fingerprint of the sample. Like a fingerprint no two unique molecular

structures produce the same infrared spectrum. This makes infrared spectroscopy useful for several types of analysis.

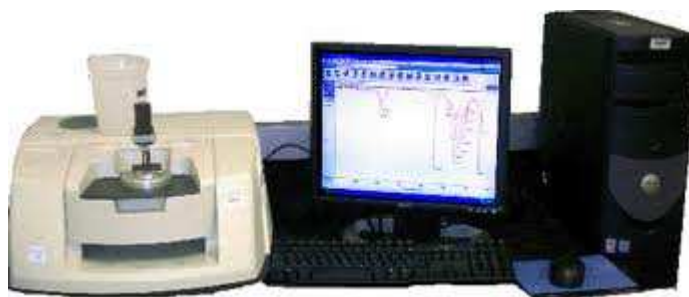The figure below shows the FTIR available in DTU:

Fig.4.10: Nicolet-380 FTIR

The goal of any absorption spectroscopy (FTIR, ultraviolet-visible ("UV-Vis") spectroscopy, etc.) is to measure how well a sample absorbs light at each wavelength. The most straightforward way to do this, the "dispersive spectroscopy" technique, is to shine a monochromatic light beam at a sample, measure how much of the light is absorbed, and repeat for each different wavelength.

The figure below shows the components of FTIR:
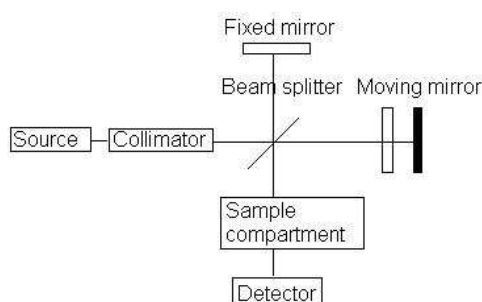
Fig.4.10: FTIR [33]

FTIR analysis can give not only qualitative (identification) analysis of materials, but with relevant standards, can be used for quantitative (amount) analysis. FTIR can be used to analyze samples up to ~11 millimetres in diameter, and either measure in bulk or the top ~1 micrometer layer.

4.2.3 Photoluminescence

Photoluminescence (abbreviated as PL) describes the phenomenon of light emission from any form of matter after the absorption of photons (electromagnetic radiation). Photoluminescence (PL) is the spontaneous emission of light from a material under optical

excitation. Features of the emission spectrum can be used to identify surface, interface, and impurity levels and to gauge alloy disorder and interface roughness. The intensity of the PL signal provides information on the quality of surfaces and interfaces [34].

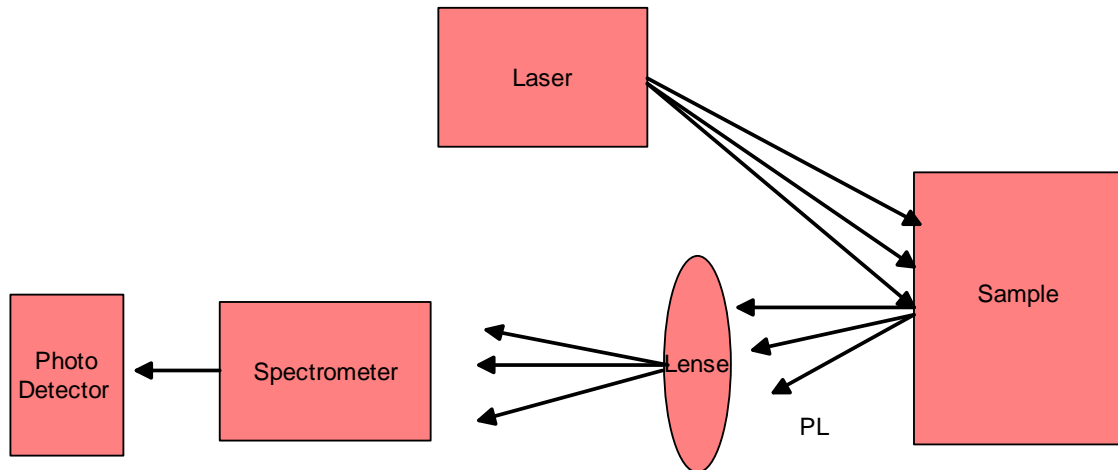Figure below shows the typical experimental set up for PL measurement.

Fig.4.11 set up for PL [34]

In a typical PL experiment, a semiconductor is excited with a light-source that provides photons with energy larger than the band-gap energy. The incoming light excites a polarization that can be described with the semiconductor Bloch equations. Once the photons are absorbed, electrons and holes are formed with finite momenta k in the conduction and valence bands, respectively. The excitations then undergo energy and momentum relaxation towards the band gap minimum. Typical mechanisms are Coulomb scattering and the interaction with phonons. Finally, the electrons recombine with holes under emission of photons.

Ideal, defect-free semiconductors are many-body systems where the interactions of charge-carriers and lattice vibrations have to be considered in addition to the light-matter coupling. In general, the PL properties are also extremely sensitive to internal electric fields and to the dielectric environment (such as in photonic crystals) which impose further degrees of complexity.

Figure below shows the PL instrument:

Fig.4.12 PL Instrument

4.4.1 HIGH RESISTANCE METER/ ELECTROMETR

An Electrometer is an electrical instrument for measuring electric charge or electrical potential difference. There are many different types, ranging from historical handmade mechanical instruments to high-precision electronic devices. In order to study electrical properties (resistance) of ZnO nano-particles electrometer/ high resistance meter is used.

Modern electrometer is a highly sensitive electronic voltmeter whose input impedance is so high that the current flowing into it can be considered, for most practical purposes, to be zero. The actual value of input resistance for modern electronic electrometers is around $10^{14}\Omega$, compared to around $10^{10}\Omega$ for nano- voltmeters.

Here we measured resistance with variation of temperature. The photograph below shows the Electrometer 6517A available in DTU.

Fig.4.14 6517A Electrometer

4.4.2 STM

The development of the family of scanning probe microscopes starts with the original invention of the STM in 1981.Gerd Binnig and Heinrich Rohrer developed the first working STM while working at IBM Zurich Research Laboratories in Switzerland. This instrument would later win Binnig and Rohrer the Nobel Prize in physics in 1986 [35]. A scanning tunnelling microscope (STM) is a non-optical microscope that works by scanning an electrical probe tip over the surface of a sample at a constant spacing. This allows for a 3D picture of the surface to be created.

The STM works by scanning a very sharp metal wire tip over a surface. By bringing the tip very close to the surface, and by applying an electrical voltage to the tip or sample, we can image the surface at an extremely small scale – down to resolving individual atoms. The STM sample must conduct electricity for the process to work. For an STM, good resolution is considered to be 0.1 nm lateral resolution and 0.01 nm depth resolution. With this resolution, individual atoms within materials are routinely imaged and manipulated. The STM can be used not only in ultra-high vacuum but also in air, water, and various other liquid or gas ambient, and at temperatures ranging from near zero Kelvin to a few hundred degrees Celsius.

In addition to scanning across the sample, information on the electronic structure at a given location in the sample can be obtained by sweeping voltage and measuring current at a specific location. This type of measurement is called scanning tunnelling spectroscopy (STS) and typically results in a plot of the local density of states as a function of energy within the sample.

Working Principle of STM

The STM is based on several principles. One is the quantum mechanical effect of tunnelling. It is this effect that allows us to "see" the surface. Another principle is the piezoelectric effect. It is this effect that allows us to precisely scan the tip with angstrom-level control. Lastly, a feedback loop is required, which monitors the tunnelling current and coordinates the current and the positioning of the tip.

Modes of Operation

First, a voltage bias is applied and the tip is brought close to the sample by coarse sample-to-tip control, which is turned off when the tip and sample are sufficiently close. At close range, fine control of the tip in all three dimensions when near the sample is typically piezoelectric, maintaining tip-sample separation W typically in the 4-7 Å (0.4-0.7 nm) range, which is the equilibrium position between attractive ($3<W<10$Å) and repulsive ($W<3$Å) interactions. In this situation, the voltage bias will cause electrons to tunnel between the tip and sample, creating a current that can be measured. Once tunnelling is established, the tip's bias and position with respect to the sample can be varied (with the details of this variation depending on the experiment) and data are obtained from the resulting changes in current.

If the tip is moved across the sample in the x-y plane, the changes in surface height and density of states cause changes in current. These changes are mapped in images. This change in current with respect to position can be measured itself, or the height, z, of the tip corresponding to a constant current can be measured. These two modes are called constant height mode and constant current mode, respectively.

In constant current mode, feedback electronics adjust the height by a voltage to the piezoelectric height control mechanism. This leads to a height variation and thus the image comes from the tip topography across the sample and gives a constant charge density surface; this means contrast on the image is due to variations in charge density. In constant height mode, the voltage and height are both held constant while the current changes to keep the voltage from changing; this leads to an image made of current changes over the surface, which can be related to charge density. The benefit to using a constant height mode is that it is faster, as the piezoelectric movements require more time to register the height change in constant current mode than the current change in constant height mode.

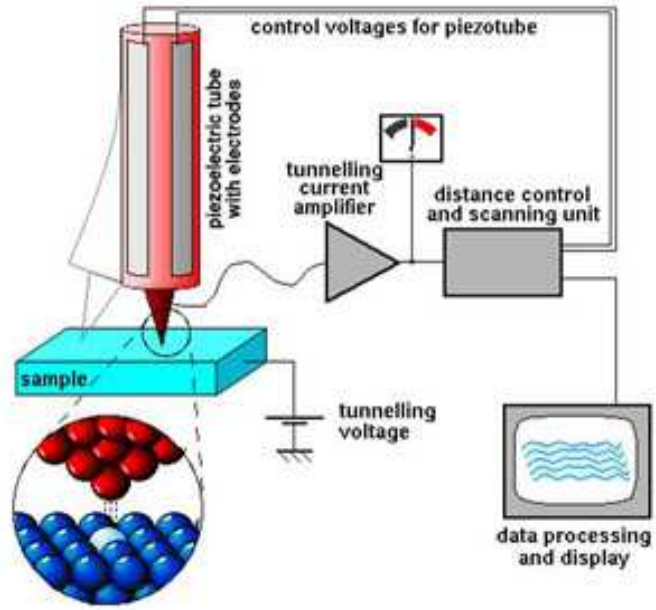The figure below shows the STM along with its components:

Fig.4.15Components of STM [8]

The photograph below shows the STM available in DTU.

Fig.4.16 STM

Chapter 5

Result and Discussion

5.1 X-ray Diffraction (XRD)

Figure.5.1 (a), (b) & (c) shows the XRD pattern of three samples calcined at 450℃, 700℃ & 900℃ respectively. Hexagonal ZnO phase (wurtzite structure) is confirmed by the study of standard data JCPDS 76-0704. Space group P63mc (186) along with hexagonal system and lattice parameters of the samples is further confirmed from XRD.
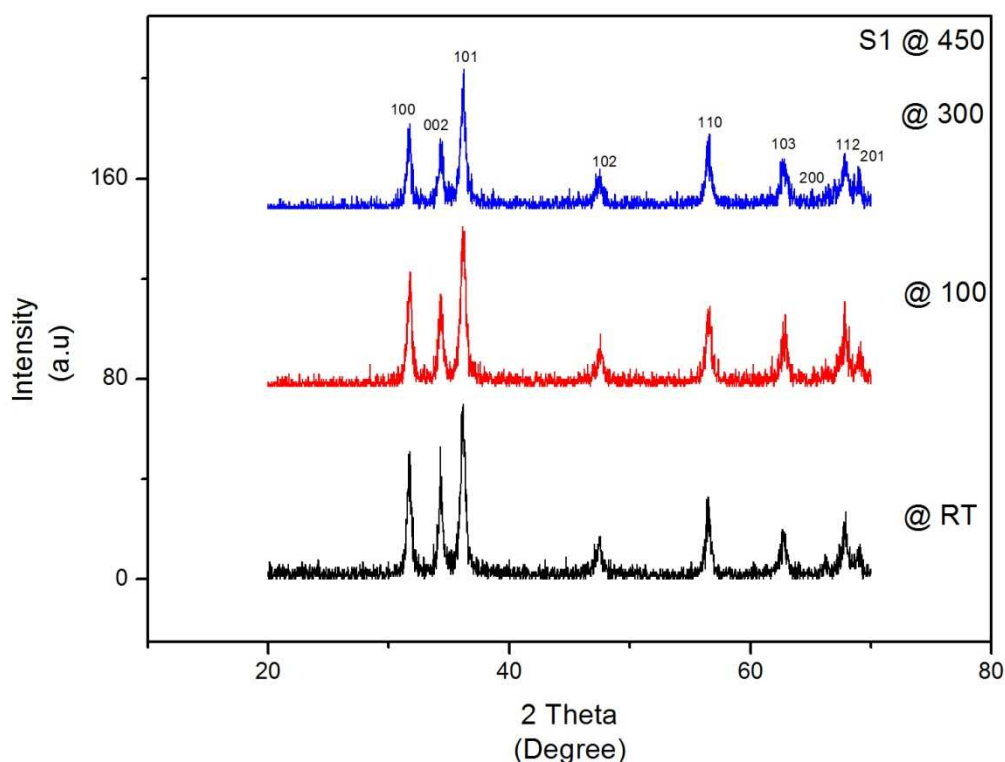
Fig.5.1 (a) XRD pattern of ZnO nanoparticles annealed @ 450℃ taken at three different temperatures to study whether there is a phase change or not
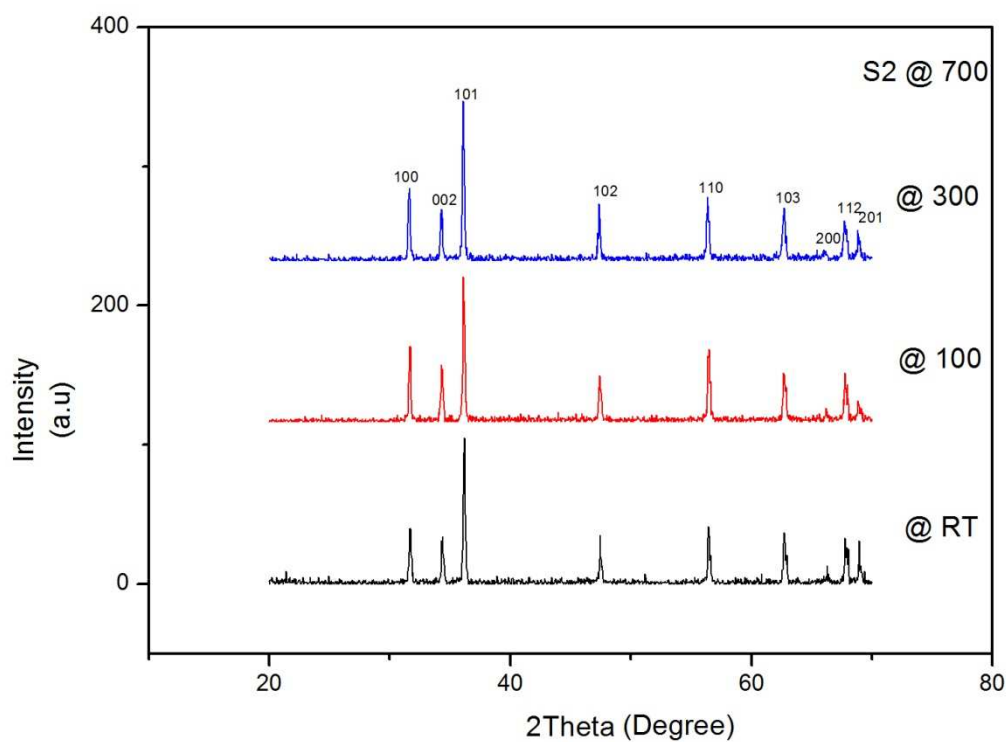
Fig. 5.1 (b) XRD pattern of ZnO annealed @ 700℃
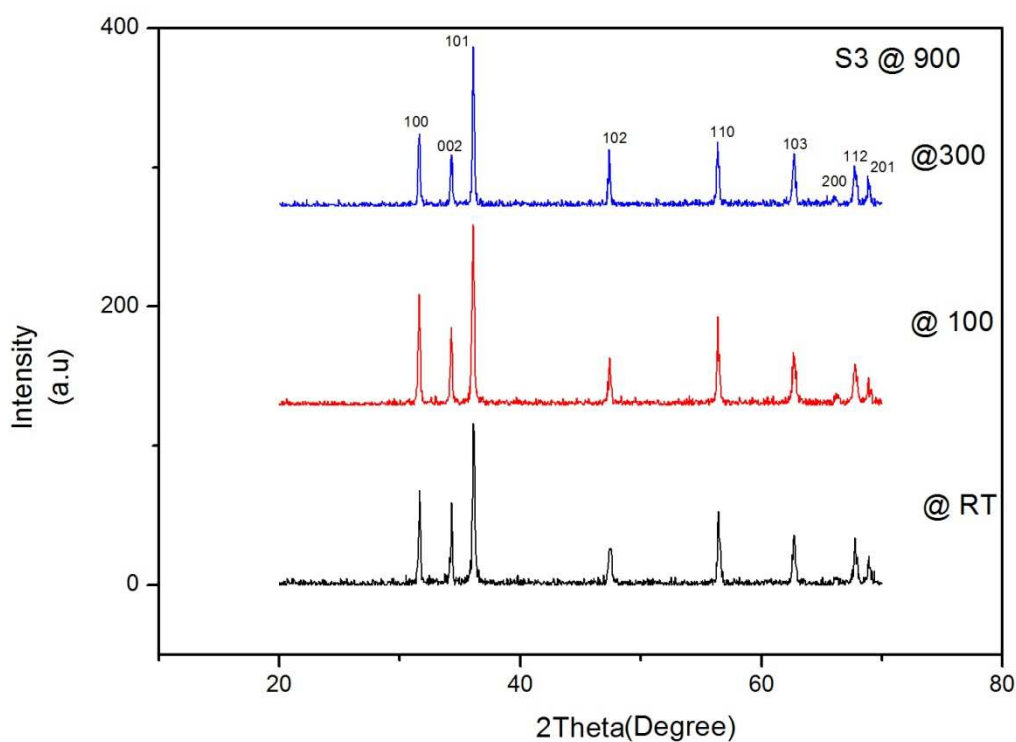
Fig. 5.1 (c) XRD pattern of ZnO nanoparticles annealed @ 900℃
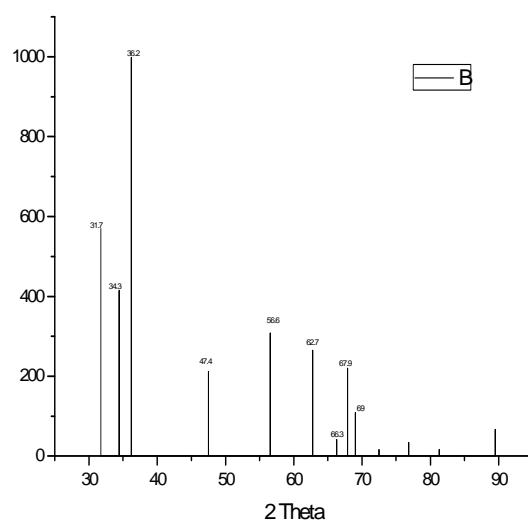
JCPDS 76-0704

The table below shows the lattice parameters of ZnO nanoparticles:

Lattice Parameter	A°
A	3.24982
C	5.20661
c/a	1.60212

Table 5.1(d) Lattice parameters of ZnO Nanoparticles determined from XRD

With increasing calcinations temperature from 450℃ to 900℃ peak height increases and FWHM decreases as a result diffraction peaks become stronger and sharper, thereby indicating that the crystal quality has been improved and the size of particles become bigger. The table below shows the variation of peak height and FWHM with different annealing temperature. The result has been shown for only high intensity peak.

	Calcination Temp ℃	Peak height	FWHM (°)
S1	450	204	0.388
S2	700	346	0.144
S3	900	385	0.113

Table 5.1 (e) shows the variation of peak height and FWHM with calcination Temperature

Table 5.1 (f), (g) and (h) below shows the % of lattice contraction at different temperatures [36]. The origin of the lattice relaxation (contraction or expansion) is due to the presence of dangling bonds in the surface layer of ZnO nanoparticles. The ions on the surface of ZnO nanoparticles are incompletely coordinated and possess the unpaired electron orbitals. Each of these dangling bonds (Zn^{2+} and O^{2-}ions) forms an electric dipole resulting in a parallel array of dipoles originating in the boundary layer of each nanoparticle lies in this surface and experience a repulsive force. ZnO has the property of adsorbing O^{2-} and O^{-}ions in the surface; hence the repulsive inter dipolar force decreases and the attractive electrostatic interaction between Zn^{2+} and O^{2-} ions increases [36]. Due to this electrostatic attraction lattice is slightly contracted.

% Variation of d with Temperature (450/300)

S.No.	2θ	$D_{observed}$	$D_{standerd}$	% contraction	(hkl)
1	31.7150	2.81231	2.81430	0.0707	100
2	34.3118	2.60289	2.60332	0.0165	002
3	36.3064	2.47483	2.47592	0.0440	101
4	47.4462	1.90982	1.91114	0.0690	102
5	56.7043	1.62451	1.62472	0.0129	110
6	62.7634	1.47604	1.47712	0.0731	103

Table 5.1 (f) % variation of 'd' at 450℃

% Variation of d with Temperature (700/300)

S.No.	2θ	$D_{observed}$	$D_{standerd}$	% contraction	(hkl)
1	31.7067	2.81290	2.81430	0.0497	100
2	34.3429	2.60027	2.60332	0.1171	002
3	36.1097	2.46938	2.47592	0.2641	101
4	47.3838	1.91080	1.91114	0.0177	102
5	56.3301	1.62094	1.62472	0.2326	110
6	62.6121	1.47151	1.47712	0.3797	103

Table 5.1(g) % variation of 'd' at 700℃

% Variation of d with Temperature (900/300)

S.No.	2θ	$D_{observed}$	$D_{standerd}$	% contraction	(hkl)
1	31.6774	2.81022	2.81430	0.1449	100
2	34.3118	2.59875	2.60332	0.1755	002
3	36.1182	2.46332	2.47592	0.5089	101
4	47.3709	1.90762	1.91114	0.1841	102
5	56.3655	1.62321	1.62472	0.0929	110
6	62.7258	1.47686	1.47712	0.0176	103

Table 5.1(h) % variation of 'd' at 900℃

The average crystallite sizes of samples S1 (450℃), S2 (700℃) and S3 (900℃) were determined by the Debye-Scherer formula. The table below shows the crystallite sizes of three samples along with Lattice constants with a variation of annealing temperature.

Zno Annealed	L (particle size) in nm	a (Lattice Constant)
450℃	20.94	3.499
700℃	56.61	3.491
900℃	71.83	3.483

Table 5.1 (i) Variation of L and a with temperature

With increasing temperature crystallinity of the particles increases causing particles become bigger. Thus,in order to get smaller particles lower temperature is favourable. And comparing the XRD report of three samples it has been concluded that samples calcined at 700 ℃ and 900 ℃ gives high intensity fine peaks, which can be used for further characterization.

In ZnO nanoparticles, there are a large number of vacancies of oxygen, vacancy clusters, and local lattice disorders present in the interface , which lead to an increase in c and

decreases in a and the volume of the unit cell. The low-temperature annealing can lead to a relaxation in the interface structure, but cannot dispel the local lattice disorders or change the internal structure of the nano-grains, so there are no apparent changes in the positions and intensities of XRD peaks. When the annealing temperature increases there

is a rapid decrease in the density of vacant lattice sites, vacancy clusters, and local lattice disorders and a rapid resumption of lattice parameters and the volume of the unit cell towards normal values, and the grains begin to grow.

Hence particle size increases with increasing temperature and lattice constant 'a' decreases with increasing temperature. For a real crystal, the calculated values of 'a' and 'c' are the same based on different crystal planes. However, the presence of a large number of vacant lattice sites and local lattice disorders may lead to serious reduction in the intensity or even the nearly disappearance of the XRD peaks of the corresponding lattice plane.

As there is no apparent change in the position of XRD peaks or disappearance of any particular peak, therefore it can be concluded that there is no phase change with increase in temperature.

The XRD patterns of the nanoparticles are considerably broadened due to the very small size of these particles. The strong and narrow diffraction peaks indicated that the product has good crystallinity.

5.2 Scanning Electron Microscope (SEM)

Figure.5.2 (a), (b) & (c) shows the SEM morphology of the synthesized nano ZnO particles at different annealing temperatures. It demonstrates clearly the formation of spherical ZnO nanoparticles, and change of the morphology of the nanoparticles with the calcinations temperature.
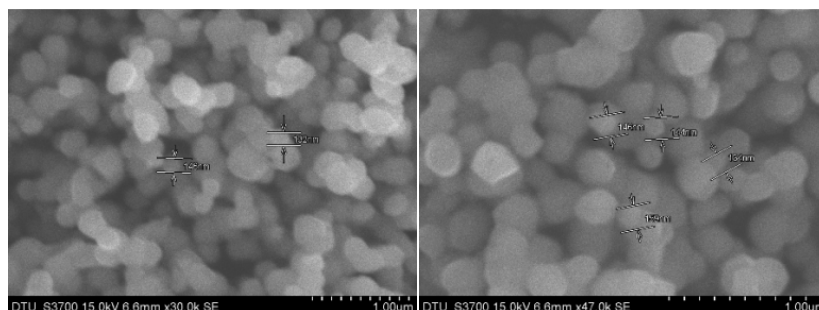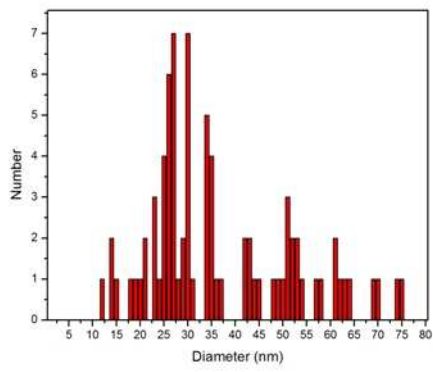
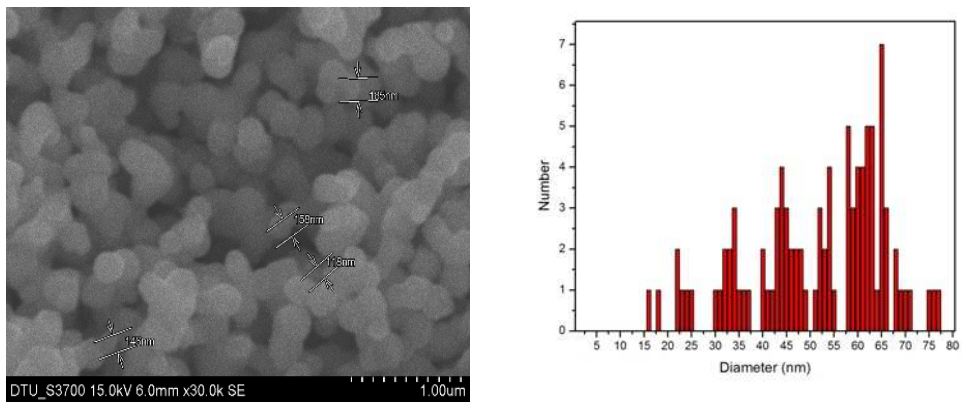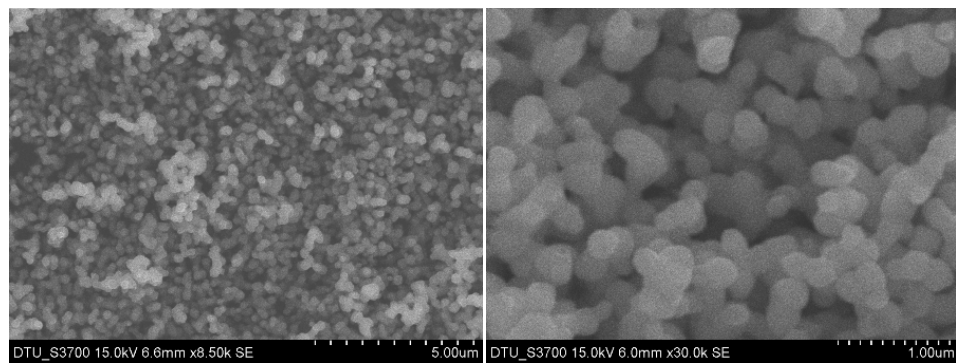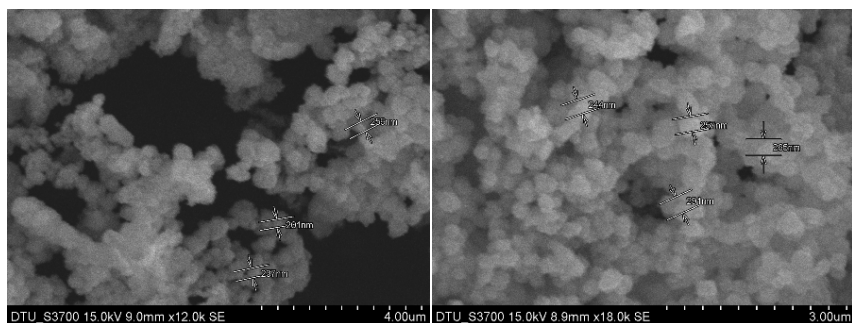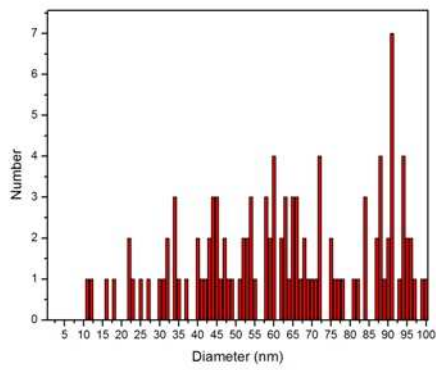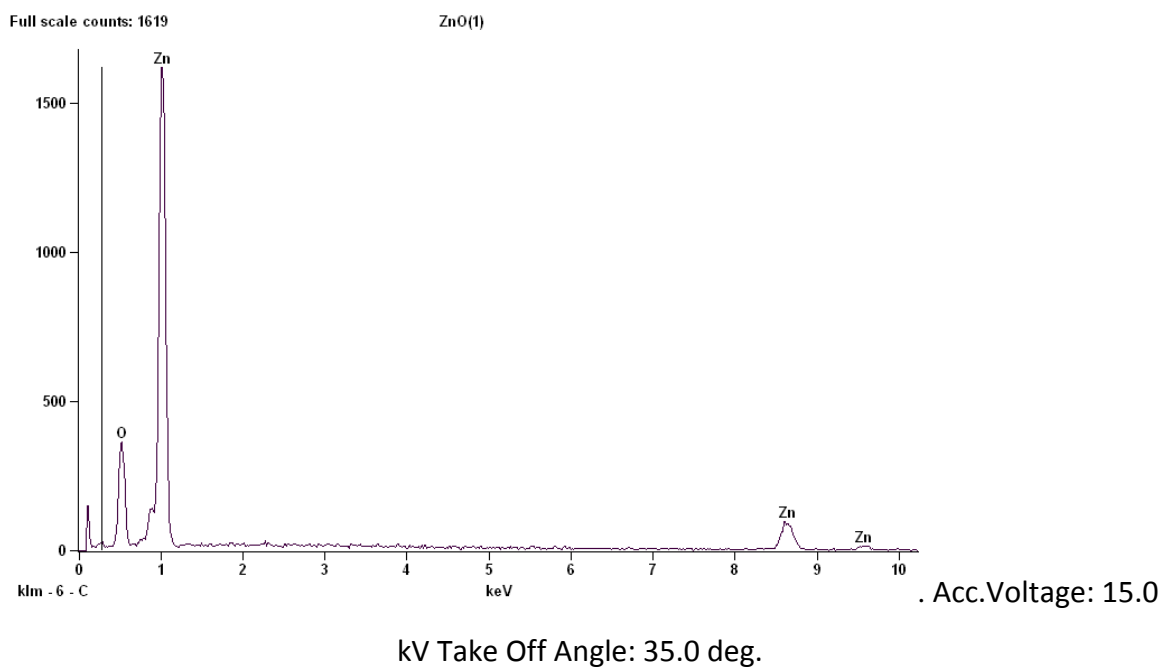Fig. 5.2 (a) SEM images of ZnO nanoparticles annealed at 450℃ for 3 hr

Fig. 5.2 (b) SEM images of ZnO nanoparticles annealed at 700℃ for 3 hr

Fig. 5.2 (c) SEM images of ZnO nanoparticles annealed at 900℃ for 3 hr

The figure below shows the EDX of ZnO sample S1

. Acc.Voltage: 15.0 kV Take Off Angle: 35.0 deg.

Quantitative Results for: ZnO(1)

Element Line	Net Counts	Int. Cps/nA	Weight %	Weight % Error	Atom %	Atom % Error	Formula	Standard Name
O K			22.99	+/- 0.46	54.96	+/-		O
	2522	0.000				1.11		
Zn K			77.01	+/- 4.26	45.04	+/-		Zn
	1538	0.000				2.49		
Zn L			---	---	---	---		
	14596	0.002						
Total			100.00		100.00			

Fig. 5.2 (d) EDX of ZnO nanoparticle annealed at 450℃

As temperature increases particles starts agglomeration which results in the formation of bigger size particles. Nucleation and growth rate increases with increase in annealing temperature, as a result agglomeration is more in the sample annealed at 900℃.

5.3 Transmission Electron Microscope (TEM)

Fig. 5.3 (a), (b) & (c) shows the TEM images of ZnO nanoparticles annealed at 450℃, 700℃ and 900℃ respectively.
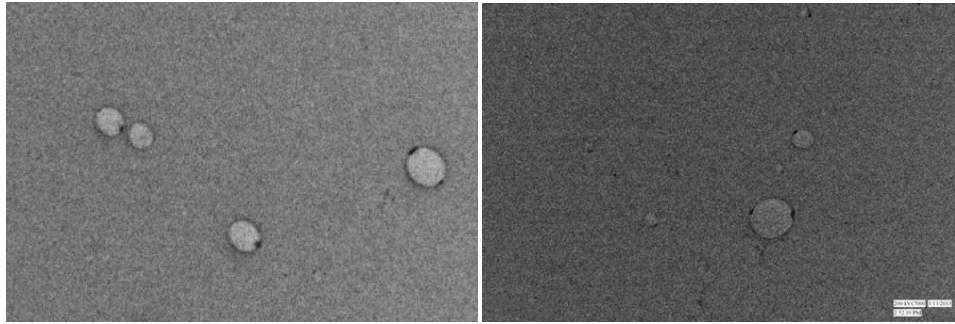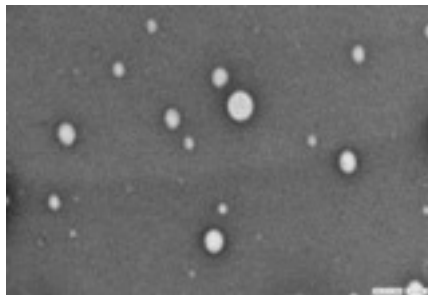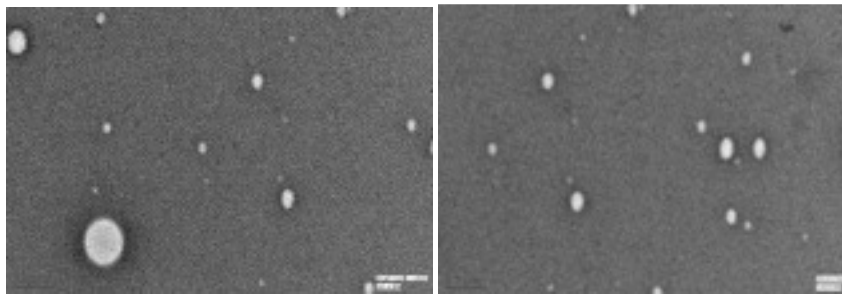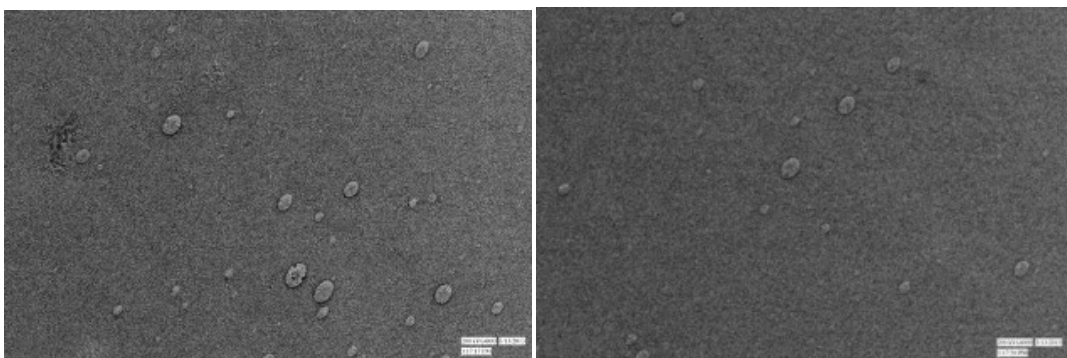
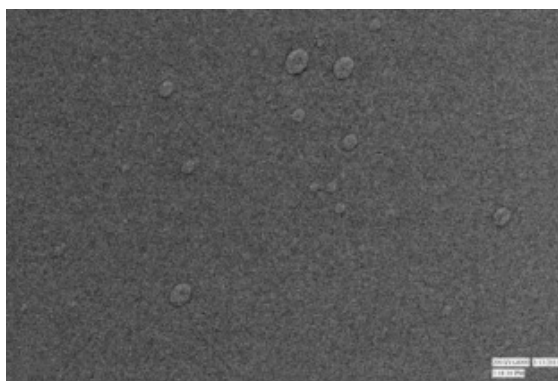Fig. 5.3 (a) TEM images @ 450 ℃

Fig. 5.3 (b) TEM images @ 700 ℃

Fig. 5.3 (c) TEM images @ 900 ℃

These images consist of spherical particles with the average size of 17 nm to 85 nm determined with the help of image J software which are in close agreement with that estimated by Scherer formula based on the XRD pattern. The table below compares the particle size determined from Debye-Scherer formula, SEM and TEM.

Temperature	XRD (nm)	SEM (nm)	TEM (nm)
450℃	20.94	26.24	16.08
700℃	56.61	62.21	60.043
900℃	71.83	90.13	84.272

Table 5.3 (d) Comparison of particle average sizes

5.4 FTIR (Fourier Transform Infrared Spectroscopy)

Fig. 5.4 shows the FTIR spectrum of the ZnO nanoparticles synthesized by wet chemical method, which was acquired in the range of 500-4000 cm^{-1}. In order to quickly establish the presence or absence of the various vibrational modes present in ZnO nanoparticle, we performed FTIR spectroscopy of ZnO nanoparticles. In order to analyze spectrum peaks are correlated with FTIR spectroscopy correlation table [40].The band 450-500 cm^{-1} correlated to metal oxide bond (Zn-O) and also authenticates presence of ZnO. The peak at 471.4 cm^{-1} is the characteristic absorption of Zn–O bond.The peaks in the range of 1000-1500cm^{-1} corresponds to the H-O-H bonding. These absorption bands are due to O-H bending of the hydroxyl group. Peak near 1640 cm^{-1}observed in sample corresponds to the C=O group carboxylic derivates, which may be due to residue of zinc acetate, is used in reaction. The adsorbed band at 3400-3500 cm^{-1} is assigned O-H stretching [39, 52, 59]. From this FTIR we can also observe that increasing the annealing temperature sharpens of

the characteristic peaks for metal oxide, sugesting that, the crystalline nature of ZnO increases on increasing the calcination temperature.
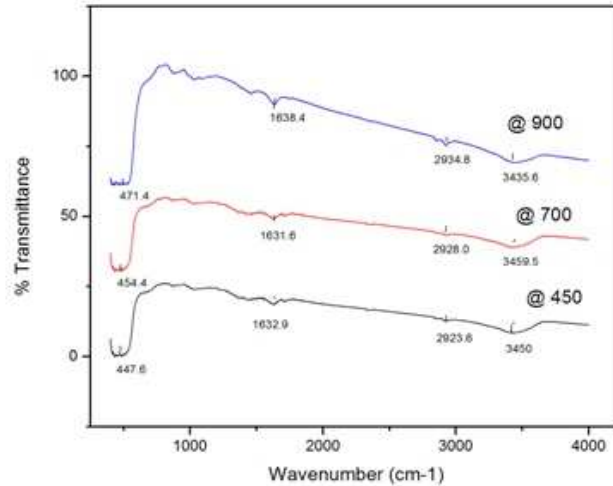

Fig. 5.4 FTIR Spectrum of ZnO nanoparticles

5.5 Ultra-Violet Visible Spectroscopy (UV-visible)

Absorption spectroscopy is a powerful non-destructive technique for exploring the optical properties of semiconducting nanoparticles. To characterize ZnO nanocrystals the sample is dispersed in ethanol solution. A blank solution of ethanol is taken in cuvette to set the baseline [40]. From the literature the absorption spectra of ZnO in the UV and visible range is observed between 350-380 nm which is a characteristic/standard peak range for a wurtzite hexagonal phase ZnO, demonstrating that the synthesized products are pure ZnO [5, 25,36, 38, 40]. It is found that the absorption edge systematically shifts to the lower wavelength or higher energy with decreasing size of the nanoparticle. This pronounced and systematic shift in the absorption edge is due to the quantum size effect [41].

5.6 Photoluminescence (PL)

The photoluminescence originates from the recombination of surface states. The strong PL implies that the surface states remain very shallow, as it is reported that quantum yields of band edge will decrease exponentially with increasing depth of surface state energy levels [41]. Figure 5.6 (a) shows the photoluminescence spectrum of ZnO nanopowder annealed at

450℃ with excitation wavelength 320 nm and 340 nm at room temperature. Figure shows three peaks from 420 nm to 500 nm (UV region) corresponding to the near band gap excitonic emission [54, 55, 57] and the other is located at around 680 nm attributed to the presence of singly ionized oxygen vacancies. The emission is caused by the radiative recombination of a photo generated hole with an electron occupying the oxygen vacancy [41]. The emission near 530 nm in ZnO is often referred as the green emission [21].
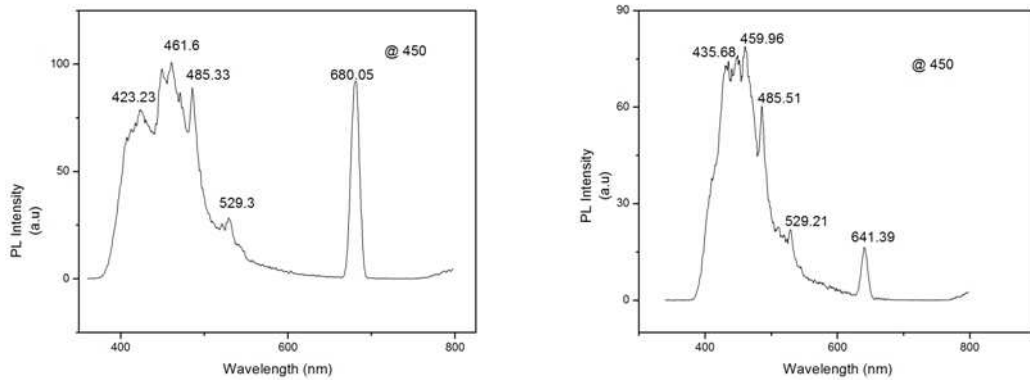

Fig 5.6 (a) PL Spectra of ZnO nanoparticles annealed at 450℃. Left one is with excitation

wavelength 320 nm and the right one is at 340 nm at 300K

The green emission is attributed to the radiative recombination of a delocalised electron close to the conduction band with deeply trapped hole.

Figure 5.6 (b) shows the PL spectra of ZnO nanopowder annealed at 700℃. From the figure it is quite clear that there is negligible change in the position of peaks in the UV region. However the intensity corresponding to oxygen vacancies is quite low. At 900℃ intensities in the UV region is low while the position of peaks remain unchanged.
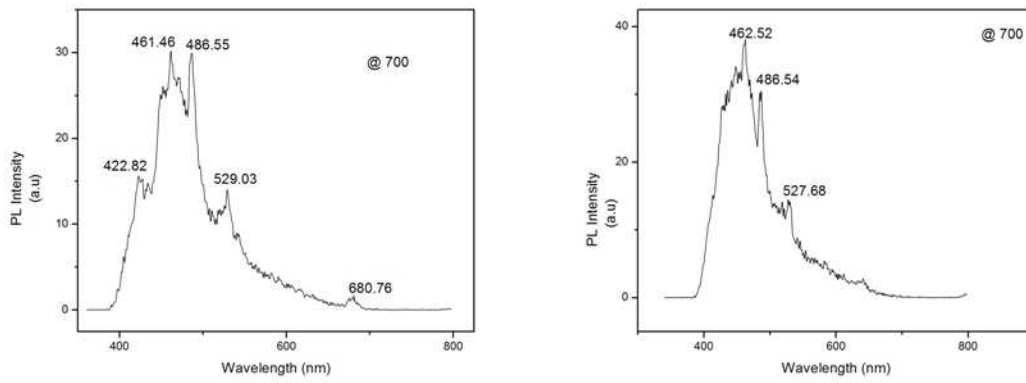
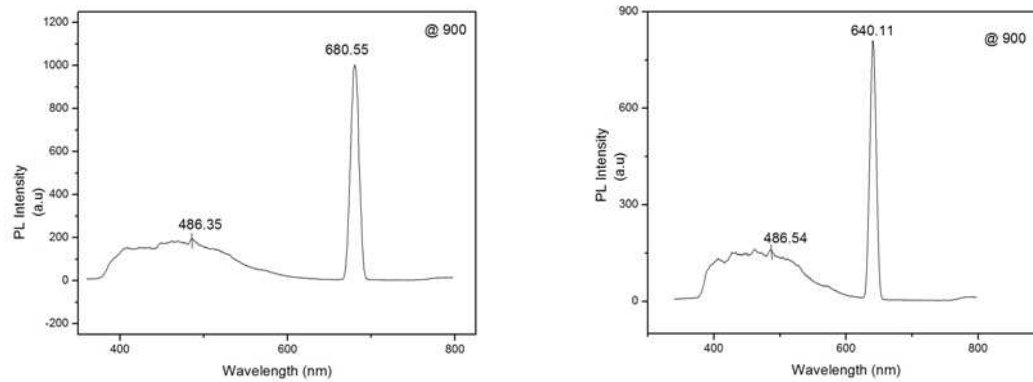Fig 5.6 (b) PL Spectra of ZnO nanoparticles annealed at 700℃

Fig 5.6 (c) PL Spectra of ZnO nanoparticles annealed at 900℃

5.8 Resistance Measurement

Figure 5.8 shows the variation of electrical resistance of ZnO nanoparticles with temperature. The decrease in resistance with increasing temperature following semiconducting behaviour of ZnO is observed.

The activation energy was determined by using the equation

$$R = R_o \exp\left(\frac{Ea}{KT}\right)$$

Where R is the resistance at temperature T, R_o is a constant, E_a is the activation energy and k is the Boltzmann constant [48].
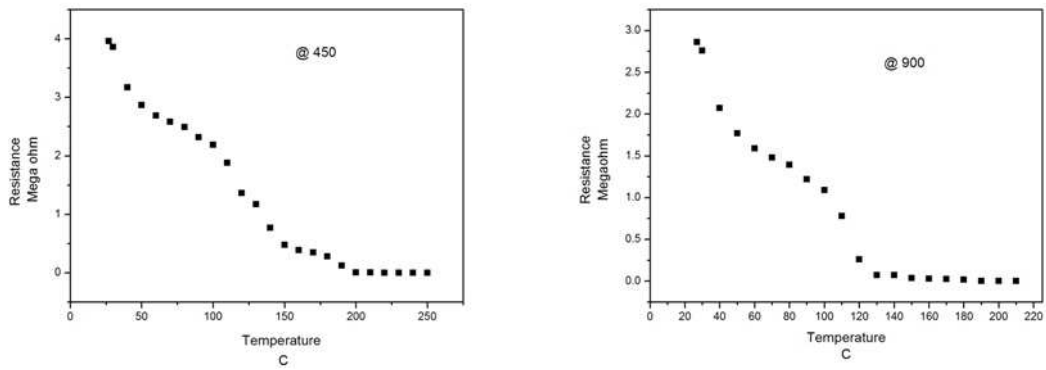
Fig. 5.8 Variation of Resistance of ZnO nanoparticles with Temperature

5.9 Scanning Tunnelling Microscope

It is used to measure correlations between the geometric structures and electrical properties of ZnO surfaces under ultra high vacuum. Tunneling spectroscopy is used to identify individual ZnO grains, grain boundaries and surface impurities [44]. Figure 5.9 (a) and (c) shows the I-V characteristics of ZnO nanoparticles made in constant current mode at Bias Voltage of -200 mV and Tunnelling current at 200 PA matches perfectly with experimental data [45, 46,47,51]. Figure 5.9 (b) and (d) shows the conductivity of the sample which matches perfectly to that of a semiconductor. Each I-V curve could be correlated to a specific point on the image. In each case the dimensionless quantity *(di/dv) / (i/v)* which has been demonstrated to be related to the local density of states [44], was obtained by numerically differentiating the experimentally determined current. When the current decreased to below the detectable limit, at biases near zero, the conductivity was defined equal to zero and the quantity (*di/dv) / (i/v)* was defined equal to one.
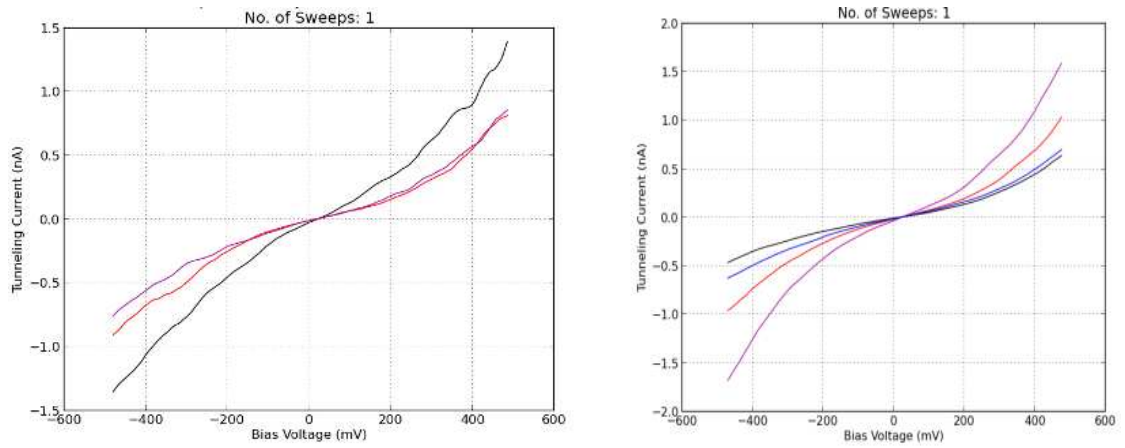

67
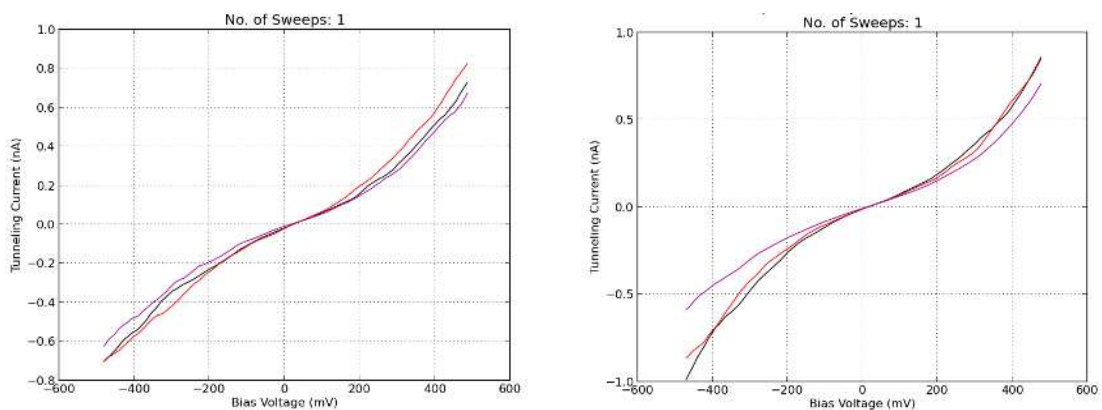
Fig. 5.9 (a) I-V characteristics of ZnO nanopowder at different points on sample annealed at 450℃
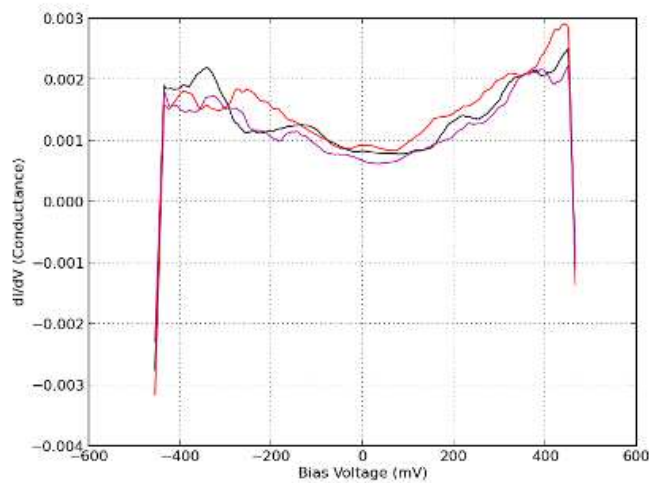

Fig. 5.9 (b) Comparison of I-V curves and conductivity for different electronic structure and the experimental obtained graph of conductivity of ZnO @ 450
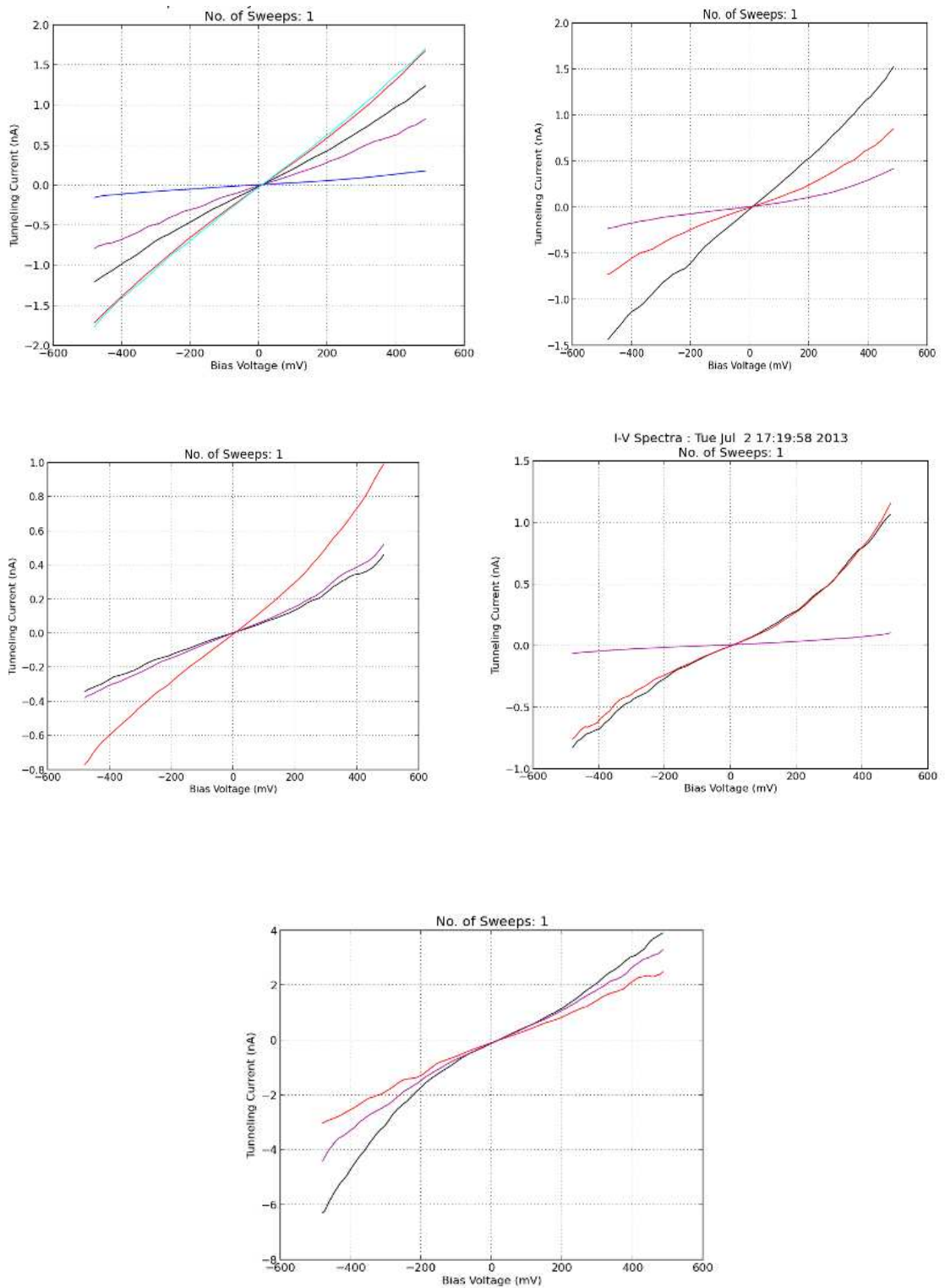
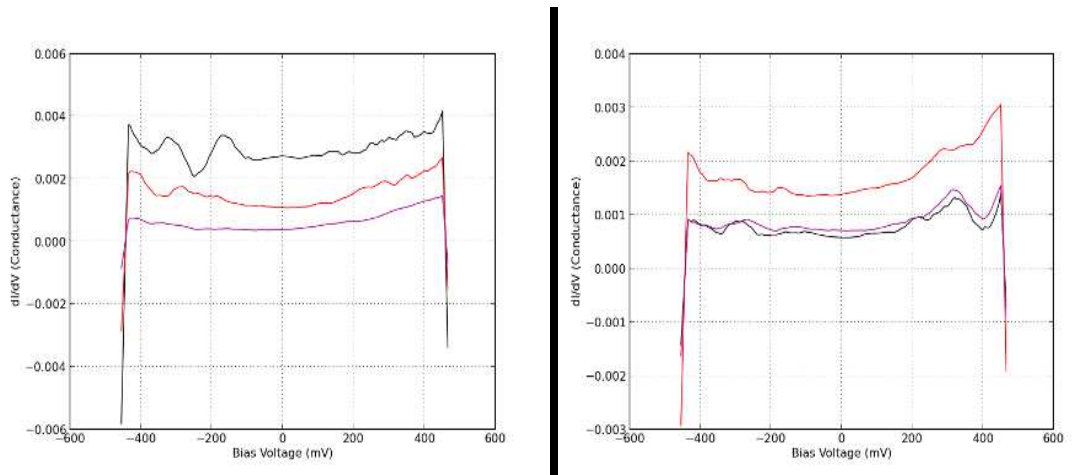Fig. 5.9 (c) I-V characteristics of ZnO nanopowder at different points on sample annealed at 900℃

Fig. 5.9 (d) Conductivity of ZnO nanoparticle at different points for 900℃

Chapter 6

Conclusion

Zinc oxide nanoparticles were synthesized through wet chemical method by considering different calcinations temperatures. The results of the XRD and TEM showed that the average particle size of ZnO particles increases with increasing calcinations temperature, and the SEM results showed that the formation of spherical shaped nanoparticles. Furthermore, the FTIR showed a broad absorption band related to Zn-O vibration band. PL shows three peaks from 420 nm to 500 nm (UV region) corresponding to the near band gap excitonic emission and the other is located at around 680 nm attributed to the presence of singly ionized oxygen vacancies. By studying variation of electrical resistance of ZnO nanoparticles with temperature semiconducting behaviour of ZnO is confirmed. The I-V characteristics of ZnO nanoparticles made in constant current mode at Bias Voltage of -200 mV and Tunnelling current at 200 PA matches perfectly with experimental data.

References

1. Anderson Janotti and Chris G Van de Walle, Rep. Prog. Phys. 72 (2009) 126501 (29pp)

2. Zhong Lin Wang, J. Phys.: Condens. Matter 16 (2004) R829–R858

3. C. W. Litton, D. C. Look, B. B. Claflin and D. C. Reynolds, R. D. Worley, Sensors Directorate, Air Force Research Laboratory (AFRUSNDM) Wright-Patterson Air Force Base, Ohio 45433, 0-7803-8614-0/04/S20.00 Q 2004 IEEE

4. R.Y. Hong, J.H. Li, D.Q. Liu, H.Z. Li, Y. Zheng, J. Ding, Powder Technology 189 (2009) 426–432

5. Shingo Tachikawa, Atsushi Noguchi, Takeharu Tsuge, Masahiko Hara, Osamu Odawara and Hiroyuki Wada, *Materials* 2011, *4*, 1132-1143; doi:10.3390/ma4061132

6. Pavan Naik , Dr. R B.Lohani,Global research Analysis Internationl,volume:2,Issue:1,Jan 2013,ISSN No 2277-8160

7. "Basics of NanoTechnology" by Horst-Gunter Rubahn

8. http//w.w.w.wikipedia.com

9. "Nanotechnology: Principles and Practices" by Sulebha Kulkarni

10. " Introduction to Nanoscience and Nanotechnology" by Gabor L. Hornyak, H.F. Tibbals, Joydeep Dutta, John J. Moore

11. K. Prasad, Anal K. Jha, Natural Science, Vol.1, No.2, 129-135 (2009)

12. Zhiyong Fan and Jia G. Lu, Zinc Oxide Nanostructures: Synthesis and Properties

13. Ling Ding, Ruixue Zhang and Louzhen Fan, Ding et al. Nanoscale Research Letters 2013, 8:78

14. Hadis Morkoç and Ümit Özgur, Zinc Oxide: Fundamentals, Materials and Device Technology. ISBN: 978-3-527-40813-9

15. Shyam Sunder Pareek, Kapil Pareek, An Empirical Study on Structural, Optical and Electronic Properties of ZnO Nanoparticles, IOSR Journal of Applied Physics (IOSR-JAP), e-ISSN: 2278-4861. Volume 3, Issue 2(March – April, 2013), PP 16-24

16. S.J. Pearton, D.P. Norton, ,K.Ip, Y.W. Heo, T. Steiner, Progress in Materials Science 50 (2005) 293–340

17. Feng Xu, Qingqun Qin, Ashish Mishra, Yi Gu, Yong Zhu, Nano Res (2010) 3: 271–280

18. Ajay Kushwaha, Himanshu Tyagi, M. Aslam, AIP Advances 3, 042110 (2013)

19. Jongmin Lim, Kyoungchul Shin, Hyoun Woo Kim, Chongmu Lee, Journal of Luminescence 109 (2004) 181–185

20. Li Wang, Yong Pu, Wenqing Fang, Jiangnan Dai, Changda Zheng, Chunlan Mo, Chuanbin Xiong, Fengyi Jiang

21. U. Pal, J. Garcia Serrano, P. Santiago, Gang Xiong, K.B. Ucer, R.T. Williams, Optical Materials 29 (2006) 65–69

22. R.E. Marotti, P. Giorgi, G. Machado, E.A. Dalchiele, Solar Energy Materials & Solar Cells 90 (2006) 2356–2361

23. C. Jagadish and S. J. Pearton, "Zinc Oxide Bulk, Thin Films and Nanostructures Processing, Properties and Application" Elsevier (2006).

24. S.C. Singh, D.P. Singh, J. Singh, P.K. Dubey, R.S. Tiwari, O.N. Srivastava, Metal Oxide Nanostructures; Synthesis, Characterizations and Applications

25. Rizwan Wahab, S.G. Ansari, Young-Soon Kim, Hyung-Kee Seo, Hyung-Shik Shin Appl. Surf. Sci., 253 (2007)622–7626.

26. Geochemical Instrumentation and Analysis, Darrell Henry, Nelson Eby, John Goodge, David Mogk

27. Geochemical Instrumentation and Analysis, Barbara L Dutrow, Louisiana State University ,Christine M. Clark, Eastern Michigan University

28. Geochemical Instrumentation and Analysis, Susan Swapp, University of Wyoming

29. Radiological and Environmental management, courtesy of Iowa State University

30. Transmission electron microscopy and diffractometry of materials by James M. Howe, Brent Fultz

31. www.nanoscience.gatech.edu

32. http://www2.chemistry.msu.edu

33. http://chemwiki.ucdavis.edu

34. Photoluminescence in Analysis of Surfaces and Interfaces, Timothy H. Gfroerer in Encyclopaedia of Analytical Chemistry R.A. Meyers (Ed.) pp. 9209–9231 John Wiley & Sons Ltd, Chichester, 2000

35. http://www.nanoscience.com

36. Optical Properties of ZnO Nanoparticles, Soosen Samuel M, Lekshmi Bose and George KC, ISSN: 0973-7464 Vol. XVI: No. 1 & 2 SB Academic Review 2009: 57-65

37. Preparation, magnetic and optical properties of ZnO and ZnO:Co rods prepared by wet chemical method, Xueyun Zhou, Shihui Ge, Dongsheng Yao, yalu Zuo, Yuhua Xiao, Journal of Alloys and Compounds 463 (2008) L9–L11

38. Synthesis and Growth of ZnO Nanoparticles, Eric A. Meulenkamp, *J.* Phys. Chem. B 1998, 102, 5566-5572

39. Low temperature dielectric studies of zinc oxide (ZnO) nanoparticles prepared by precipitation method, Amrut S. Lanje, Satish J. Sharma, Raghumani S. Ningthoujam, J. S. Ahn, Ramchandra B. Pode, Advanced Powder Technology, Volume 24, Issue 1, January 2013, Page 331-335

40. Preparation of ZnO nanoparticles by solvothermal process, Amritpal Singh, Rajesh Kumar,Mrs. Neeru Malhotra, Suman, International Journal for Science and Emerging, Technologies with Latest Trends" 4(1): 49-53 (2012)

41. Synthesis, Characterization, and Spectroscopic Properties of ZnO Nanoparticles, Satyanarayana Talam, Srinivasa Rao Karumuri, Nagarjuna Gunnam, ISRN Nanotechnology Volume 2012 (2012), Article ID 372505, 6 pages

42. The crystallization and physical properties of Al-doped ZnO nanoparticles, K.J. Chen, T.H. Fang, F.Y. Hung, L.W. Ji, S.J. Chang, S.J. Young, Y.J. Hsiao, Applied Surface Science 254 (2008) 5791–5795

43. Synthesis and Characterization of ZnO Nano-Particles, C. A. Omondi, T. W. Sakwa, Y. K. Ayodo, K. M. Khanna, International Journal of Physics and Mathematical Sciences ISSN: 2277-2111

44. Electrical Properties of individual ZnO grain boundaries determined by spatially resolved tunnelling spectroscopy, Gregory S. Rohrer, Dawn A. Bonnell, J. Am. Ceram. Sac. 73 [10], 3026-32 (1990)

45. Power Generating Characteristics of Zinc Oxide Nanorods Grown on a Flexible Substrate by a Hydrothermal Method, Jae-hoon Choi, Xueqiu You, Chul Kim,

Jungil Park, James Jungho Pak, Journal of Electrical Engineering & Technology Vol. 5, No. 4, pp. 640~645, 2010

46. Thickness dependence of the structural and electrical properties of ZnO thermal-evaporated thin films, A Ghaderi, S M elahi, S Solaymamni, M Naseri, M Ahmadirad, S Bahram, A E Khalili, Pramana— journal of physics, Indian Academy of Sciences Vol. 77, No. 6, December 2011, pp. 1171–1178

47. Electron transport properties in ZnO nanowires/poly(3-hexylthiophene) hybrid nanostructure, Ke Cheng, Gang Cheng, Shujie Wang , Dongwei Fu, Bingsuo Zou, Zuliang Du, Materials Chemistry and Physics 124 (2010) 1239–1242

48. Preparation of Al-doped ZnO (AZO) Thin Film by SILAR, S. Mondal, K. P. Kanta and P. Mitra, Journal of Physical Sciences, Vol. 12, 2008, 221-229

49. Synthesis by Wet Chemical Method and Characterization of Nanocrystalline ZnO Doped with Fe2O3, U. Narkiewicz, D. Sibera, I. Kuryliszyn-Kudelska, L. Kilanski, W. Dobrowolski, N. Rom·cevic, Vol. 113 (2008) ACTA PHYSICA POLONICA A No. 6

50. ZnO NANOPARTICLES AND THEIR APPLICATIONS – NEW ACHIEVMENTS, Dušan NOHAVICA and Petar GLADKOV, 12. - 14. 10. 2010, Olomouc, Czech Republic, EU

51. Temperature Dependant Structural and Electrical Properties of ZnO Nanowire Networks, S. Al-Heniti, R. I. Badran, A. Umar, A. Al-Ghamdi, S. H. Kim, F. Al-Marzouki, A. Al-Hajry, S. A. Al-Sayari, and T. Al-Harbi, Journal of Nanoscience and Nanotechnology Vol. 11, 1–7, 2011

52. Room Temperature Synthesis of ZnO Quantum Dots by Polyol Methods, Rongliang He and Takuya Tsuzuki, Centre for Frontier Materials Deakin University, Geelong Technology Precinct, Geelong, VIC, Australia

53. ZnO nanorods and nanopolypods synthesized using microwave assisted wet chemical and thermal evaporation method, A.K Singh, S S Multani, S B Patil, Indian Journal of Pure & Applied Science, Vol. 49, April 2011, pp. 270-276

54. Chemical Synthesis and Visible Photo-Luminescence Emission From Monodispersed ZnO Nanoparticles, P. Kumbhakar*, D. Singh, C. S. Tiwary, and A. K. Mitra, Chalcogenide Letters Vol. 5, No. 12, December 2008, p. 387 – 394

55. Well-integrated ZnO nanorod arrays on conductive textiles by electrochemical synthesis and their physical properties, Yeong Hwan Ko, Myung Sub Kim, Wook Park and Jae Su Yu, Ko et al. Nanoscale Research Letters 2013, 8:28

56. Threading dislocations in domain-matching epitaxial films of ZnO, W.-R. Liu, W. F. Hsieh,C.-H. Hsu, Keng S. Liang, F. S.-S. Chien, Journal of Applied Crystallography ISSN 0021-8898

57. Biological approach of zinc oxide nanoparticles formation and its characterization , Ravindra P. Singh*, Vineet K. Shukla, Raghvendra S. Yadav, Prashant K. Sharma, Prashant K. Singh, Avinash C. Pandey, Adv. Mat. Lett. 2011, **2**(4), 313-317

58. Synthesis, Characterization, and Applications of ZnO Nanowires, Yangyang Zhang,Manoj K. Ram, Elias K. Stefanakos, and D. Yogi Goswami, Journal of Nanomaterials, Volume 2012, Article ID 624520, 22 pages

59. Synthesis of ZnO Nanoparticles by Spray Pyrolysis Method Ghaffarian, Hamid Reza, Saiedi, Mahboobeh, Sayyadnejad, Mohammad Ali, Iran. J. Chem. Chem. Eng. Vol. 30, No. 1, 2011

60. Preparation and Characterization of ZnO and Mg-ZnO nanoparticle R. Viswanatha, T.G. Venkatesh, C.C. Vidyasagar, Y. Arthoba Nayaka, Archives of Applied Science Research, 2012, 4 (1):480-486